

Characterizing the Risk of Atrial Fibrillation in Cardiac Patients with Exceptional Electrocardiogram Phenotypes

Lieke van den Biggelaar
l.a.j.v.d.biggelaar@tue.nl
Eindhoven University of Technology
Eindhoven, the Netherlands

Arthur Bouwman
arthur.bouwman@catharinaziekenhuis.nl
Catharina Hospital
Eindhoven, the Netherlands

Rianne M. Schouten
r.m.schouten@tue.nl
Eindhoven University of Technology
Eindhoven, the Netherlands

Ashley de Bie
ashley.d.bie@catharinaziekenhuis.nl
Catharina Hospital
Eindhoven, the Netherlands

Wouter Duivesteijn
w.duivesteijn@tue.nl
Eindhoven University of Technology
Eindhoven, the Netherlands

Abstract

We provide a transparent method to characterize Atrial Fibrillation (AF) caused by cardiac surgery, using Electrocardiogram (ECG) phenotypes. Current practice in the hospital is reactive rather than preventive and is based on a third party's proprietary alarms on vitals. Assistance with detection and prediction methods often lacks sufficient insights into their decisions toward the users, i.e., the hospital workers. This aspect is necessary to gain the trust of medical workers and patients in the decisions that are made. Our objective of transparently identifying risk factors for AF helps experts increase their understanding of the problem, and assists in decision-making about administering preventive medication to risk groups. With the deployment of the Exceptional Model Mining (EMM) framework on AF-related ECG phenotypes, we introduce a transparent and actionable method that assists the hospital in preventive treatment. We find several subgroups with EMM that align with known risk factors in the existing literature, confirming the ability of our method to identify risk groups of AF successfully. In addition, new hypotheses on found characteristics and combinations thereof have originated from the deployment. The hospital is advised to administer preventive medications to patients that match the descriptions of the risk groups found.

CCS Concepts

• Information systems → Data mining; Association rules; • Computing methodologies → Cluster analysis; Anomaly detection; Artificial intelligence.

Keywords

Atrial Fibrillation, Electrocardiogram Signals, Exceptional Model Mining, Signal Processing

Permission to make digital or hard copies of all or part of this work for personal or classroom use is granted without fee provided that copies are not made or distributed for profit or commercial advantage and that copies bear this notice and the full citation on the first page. Copyrights for components of this work owned by others than the author(s) must be honored. Abstracting with credit is permitted. To copy otherwise, or republish, to post on servers or to redistribute to lists, requires prior specific permission and/or a fee. Request permissions from permissions@acm.org.

KDD '25, August 03–07, 2025, Toronto, Canada

© 2025 Copyright held by the owner/author(s). Publication rights licensed to ACM.
ACM ISBN 978-1-4503-XXXX-X/18/06
<https://doi.org/XXXXXXX.XXXXXXX>

ACM Reference Format:

Lieke van den Biggelaar, Rianne M. Schouten, Ashley de Bie, Arthur Bouwman, and Wouter Duivesteijn. 2025. Characterizing the Risk of Atrial Fibrillation in Cardiac Patients with Exceptional Electrocardiogram Phenotypes. In *Proceedings of the 31st ACM SIGKDD Conference on Knowledge Discovery and Data Mining (KDD '25)*. ACM, New York, NY, USA, 17 pages. <https://doi.org/XXXXXXX.XXXXXXX>

1 Introduction

Atrial Fibrillation (AF) is a cardiac arrhythmia that can be a side effect of cardiac surgery [1]. Up to 50% of cardiac patients develop AF within the first four weeks after surgery [44]. Once a patient has experienced AF, episodes can come and go for the remainder of their life. The resulting heart rhythm disturbance leads to turbulent blood flow, which can cause blood clots. A stroke is the main consequence of these blood clots [40]: 20% of AF patients get a stroke, making AF its leading cardiac cause [18]. AF episodes can be cured, but the risk of future episodes remains. AF occurrence can be prevented with medication, thereby preventing risks introduced by AF [37]. The value of our method lies in identifying the risk groups of AF for which doctors can administer these preventive medications.

Current practice is reactive rather than preventive [37]. Monitoring systems are installed in the Intensive Care Unit and Operating Rooms to record vitals and are equipped with alarms. These systems are created by a third party, using proprietary methods: alarms are triggered by variations in Electrocardiogram (ECG) signals whose properties are unknown to the users, i.e. the hospital workers. This method is sufficient to help patients who experience AF, but as the episode is already occurring, preventive medication cannot be administered. Predictive methods have been applied to assist doctors in dividing ECG features, and detecting and predicting AF [6, 20, 59]. This is possible due to the phenotypes in the ECG signals such as irregular Heart Rate Variability (HRV) and the absence of P-waves (more details to follow in Section 2). These solutions generally fall under the global modeling paradigm within data mining: one model is trained to make a prediction for every patient in the current data set and every new patient that might still emerge later. This one-size-fits-all approach is common: we learn a model, striving for a high predictive accuracy that generalizes to unseen examples, and then deploy that model globally. It is well-known, however, that this is not necessarily the correct approach in medicine [12]. To build trust between the deployed methods and the users, i.e., the medical workers, and to comply with ethical considerations about

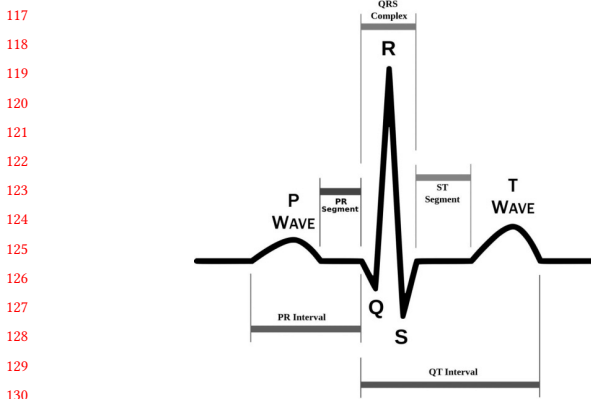


Figure 1: The ECG signal of one cardiac cycle showing each component in the PQRST-complex [5].

the sensitive healthcare application, we should ensure that patients receive the care that is correct for them. In a move towards stratified medicine [55] we develop and deploy a method that can identify subgroups of patients with a higher risk of developing AF during or after surgery, aimed at detecting combinations of risk factors. With this information, doctors can provide preventive medications rather than curative treatment.

A suitable method for stratified medical assistance is Exceptional Model Mining (EMM) [16, 35]. EMM aims to identify actionable subgroups that show exceptional behavior, such as phenotypes on the ECG that indicate AF. Existing EMM methods are commonly applied to tabular representations of the data. However, our research concerns time-varying data: time series in the form of ECG signals and their characteristics. We address in this paper the challenge of adapting existing EMM methods to fit our data type.

The deployment of our method in the Catharina hospital in Eindhoven, the Netherlands has resulted in the discovery of various risk groups that are defined in terms of patient characteristics and have exceptional morphologies in their ECG. These subgroups align with existing literature, thus confirming the validity of our approach. We find several surprising risk group characteristics and combinations thereof that are interesting to research as hypotheses in future work on AF risk factors. Our results assist the hospital workers in determining the need for preventive medication for patients described by the subgroups.

This research contributes to the field of AF analysis and EMM. Our contribution includes (1) the deployment of EMM in the hospital to characterize AF, (2) the finding of previously unknown potential risk groups for AF during and after surgery, (3) the application of EMM on ECG signals (time series), (4) the introduction of new quality measures based on ECG phenotypes, and (5) the evaluation of the validity of subgroups using additional medical characteristics.

2 AF Background and Related Work

The process of pumping blood through the body, the *cardiac cycle*, works with pressure variations activated by an electrochemical pulse [28]. Every individual has a unique rhythm of the cardiac

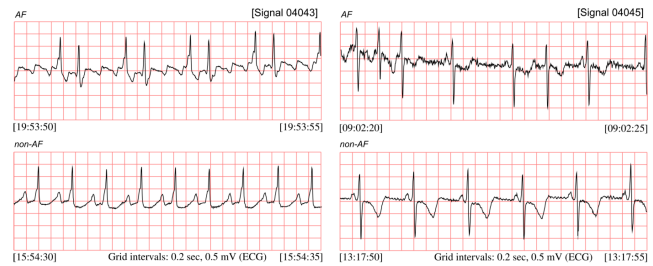


Figure 2: A visual representation of the ECG morphology of AF (top) and sinus (bottom) rhythms of two patients [15].

cycle, the *heart rhythm*, suitable for their body type and lifestyle, adapting to daily activities by increasing or decreasing the frequency of cardiac cycles, the *heart rate*.

We monitor the heart rate by measuring its electrochemical activity, through an *Electrocardiogram* (ECG). Using up to twelve leads, we record several angles resulting in different morphologies of this activity [41]. The signals are complex waveforms of elements, typically modeled as a *PQRST-complex*; Figure 1 displays an example. This model imitates the heart in one cardiac cycle.

Atrial Fibrillation (AF) is a heart arrhythmia that is often triggered after cardiac surgery. It is caused by a dysfunction in the node that gives the electrochemical pulse to activate the cardiac cycle. AF patients receive this signal through pulses originating outside of the sinoatrial node. These rapid pulses cause the atria, the heart's upper chambers, to fibrillate [28]. AF can be identified by variations in the morphology of the ECG, the *phenotypes*, as shown in Figure 2. The four diagrams represent two ECGs typical of AF (top row), and two ECGs of those same patients as a sinus rhythm (bottom row). While it is obvious that the top diagrams represent a higher degree of irregularity than the bottom diagrams, it is also obvious that the diversity of signals between patients provides a challenge for extracting the AF-relevant aspects from ECGs. P-waves represent the electrochemical signal, whose absence in AF causes the absence of the P-wave in the ECG. As a consequence, a sequence of impulses can be generated in the heart that mimics the absent signal, causing fibrillatory waves (F-waves) to form between the T-wave and the QRS-complex [26]. The other visible phenotype is irregular Heart Rate Variability (HRV), shown by the RR-intervals. The duration of the RR-interval varies from the beginning to the end of an episode of AF, making it a consequence of AF rather than a precursor [51].

2.1 Predictive Methods

With new technologies, AF can be detected without continuous manual monitoring or third-party alarms. A simple method uses statistical analysis on the PQRST-complex in ECG signals [54]. Improvements to this method include more complex frameworks based on the irregularities in the signals found using pattern analysis based on various phenotypes, such as RR-intervals [33] or missing P-waves [13]. These models can be based on autoregressive moving average models [33], hidden Markov models [13], and neural networks [10].

AF detection focuses on the phenotypes indicating AF, while prediction algorithms must find abnormalities in the ECG before

AF. These algorithms use various characteristics in frequency, time, space, and other nonlinearities modeled using a support vector machine [9], random forest, multilayer perceptron, and k-nearest neighbor [50]. Many more applications of detection and prediction algorithms exist; a good survey can be found in [32]. The detection and prediction algorithms achieve great accuracy, but in a global, one-size-fits-all manner that befits data mining really well but may not be the best approach for healthcare [12]. This complicates the deployment of these predictive methods in real-world practice.

2.2 Descriptive Methods

As opposed to the global modeling exemplified by predictive methods, another class of methods takes a local view of the data set, striving to describe only part of the data set at a time. This setting falls under the umbrella of *Local Pattern Mining* (LPM) [46]: inherently transparent methods leading to the discovery of interesting subgroups in the data set. *Frequent Itemset Mining* (FIM) [4] is such a transparent method that aims to discover combinations of items that occur frequently in the data. Such itemsets are turned into rules in *Association Rule Learning* (ARL) [4]: if all items on the left-hand-side of the rule are present in a transaction, often, so are all items on the right-hand-side. FIM and ARL are *unsupervised* variants of LPM: all items play the same role in the algorithm and can in principle appear on both sides of the arrow. *Supervised* alternatives also exist in LPM: these partition the attributes of a data set in *descriptors* (LHS) and *targets* (RHS). *Subgroup Discovery* (SD) [31, 58] strives to find subgroups where a single target column has an exceptional distribution. *Exceptional Model Mining* (EMM) [16, 35] generalizes SD to a more complex target space: it seeks subgroups where some modeling over a target space displays exceptional behavior.

2.2.1 Application on AF. ARL is used to analyze stroke risks [29] and to detect cerebral infarction in patients with AF [38]. In the former AF is included as a descriptor and the latter includes AF as a population requirement. An instance of SD similarly uses AF as a descriptor to find subgroups of patients with brain injury [20]. FIM is applied to identify risk factors for strokes in episodes of AF [39] and discover improvements in stroke preventive treatments after AF [24]. They aim to identify patients at risk for strokes out of a population of patients who have or had AF. Lastly, clustering is used to distinguish various types of AF experienced by patients [47, 56], finding various risk factors in the population of patients who all experienced AF.

3 Preliminaries: the EMM Framework

Assume a data set Ω , which is a bag of N patients $p \in \Omega$ of the form $p = (a_1, \dots, a_M, \ell_1, \dots, \ell_K, b_1, \dots, b_L)$. Here, (a_1, \dots, a_M) are the M *descriptors*, taking values from the domain $\mathcal{A} = \bigtimes_{i=1}^M \mathcal{A}_i$, where the product is a Cartesian product and each \mathcal{A}_i can be any reasonable domain: integer values if a_i represents age, continuous values if a_i represent some sensor reading, categorical values if a_i represents smoking history, and so on. Collectively, \mathcal{A} represents the Electronic Health Records (EHR). The attributes (ℓ_1, \dots, ℓ_K) are the numeric and binary representations of the phenotypes of AF in the ECG, referred to as *targets*. Lastly, binary AF complication occurrences at L stages (b_1, \dots, b_L) are used to evaluate subgroups.

Specifics are indicated with superscript and subscript: patient j with attribute a_m^j about characteristic m .

Candidate subgroups are generated by a guided search through a *description language* \mathcal{D} , encompassing several *descriptions* $D \in \mathcal{D}$. Mathematically, a description can be any function $D : \mathcal{A} \rightarrow \{0, 1\}$. In practice, \mathcal{D} is typically limited to conjunctions of conditions on individual descriptors a_i : a description will take a form such as “age ≤ 25 AND smokes = true”. Descriptions, in turn, induce subgroups.

Definition 3.1 (Subgroup). The *subgroup* induced by a description D is the bag of patients $G_D \subseteq \Omega$ such that

$$G_D = \left(p^j \in \Omega \mid D(a_1^j, \dots, a_M^j) = 1 \right)$$

Candidate subgroups are evaluated through a *quality measure* φ .

Definition 3.2 (Quality Measure). A *quality measure* (QM) is a function $\varphi : \mathcal{D} \rightarrow \mathbb{R}$ assigning a numerical value to description D .

The QM quantifies the extent to which model behavior in the target space of subgroup G_D varies from that same behavior across the entire data set Ω . Subsequently, the goal of Exceptional Model Mining is to report a list of exceptional subgroups (task definitions vary: top- k , top- k under diversity constraints, all subgroups passing a significance test, etcetera), discovered in a search through the space of candidate subgroups (strategies vary: BFS, DFS, Beam Search, etcetera) guided by φ .

4 Cardiac Signal Preprocessing

Recorded signals suffer from distortions and faults that mask the underlying patterns. Noise in ECGs can be caused by power line interference, muscle artifact, baseline wander, and human error [30]. The leads can even be incorrectly secured, leading to inverted signals. This noise sabotages our analysis and needs to be handled while keeping the underlying signal intact. Several signal processing steps are applied to overcome such noise.

First, we apply an altered version of NeuroKit ECG inversion [42, 43]: it checks if a waveform is inverted, and if so, inverts it back. Their backup check is removed for efficiency benefits.

The remaining signal noise can be categorized into *frequency noise* and *artifact noise*. Frequency noise obstructs patterns in heart rhythms, interfering with AF phenotypes. This operates at high frequencies: 50–60 Hz and over 100 Hz [48]. Artifact noise obstructs the small variations in the ECG signals by creating fluctuations around the baseline below 1 Hz [36]. Both can be removed by a filter that cuts off either high or low frequencies.

We test several denoising methods. We implement discrete wavelet transform methods using wavelets with a curve similar to the PQRST-complex. The Daubechies3 [7] and Symlet3 [11] wavelets tend to overfit, leaving noise in the signal. The Biorthogonal4.4 [2] wavelet recreates sinus rhythms, which removes the irregular AF phenotypes in the ECG. Other filters include the Butterworth [8] band-pass filter which smooths the signal and lowers the peak amplitudes. Low-pass filtering tends to over-smooth the peaks leaving them undetectable, and high-pass filtering amplifies the peaks out of proportion, doing the same for peaks caused by noise. The Weighted Moving Average (WMA) [49] filter removes noise while keeping the form of the signal. A combination of Butterworth high-pass and Gaussian WMA filters proves to be the best. Butterworth

Table 1: The ECG characteristics of the sinus rhythm and four heart arrhythmia with similar variations in the ECG: Atrial Fibrillation (AF), Ventricular Fibrillation (VF), Atrial Flutter (AFl), and Left Bundle Branch Block (LBBB).

Rhythm	RR-interval	P-wave	T_{QRS}
<i>Sinus</i>	regular	constant	60–100 ms
<i>AF</i>	irregular	non-existent	< 120 ms
<i>VF</i>	irregular	AV-dissociation	> 120 ms
<i>AFl</i>	regular	negative saw-tooth	< 120 ms
<i>LBBB</i>	irregular	non-existent	> 120 ms

high-pass eliminates baseline wander with a cutoff at 0.75; a value closest to the frequency of baseline wander, while keeping a buffer for weaker recordings. Gaussian WMA over ten instances with a sigma of 20 removes the remaining noise. These settings eliminate the noise in the signal while keeping its features close to the original. The resulting ECG signal contains clear and smooth heartbeats while keeping the AF phenotypes intact. Recordings under 30 seconds are removed: they risk having much noise compared to the number of features in the signal.

4.1 Distinguishing Arrhythmia Types

We identify ECG characteristics that separate AF episodes from sinus rhythms and other arrhythmias. These characteristics are irregular RR-intervals and P-wave absence (cf. Section 2).

A sinus rhythm features a heart rate of 60–100 bpm, PQ-intervals of 120–200 ms, QRS-complexes of 60–100 ms, and a P-wave duration of up to 120 ms [14]. Heart arrhythmias are identifiable by variations of these characteristics. Table 1 lists four arrhythmias with similar morphological abnormalities. Ventricular Fibrillation (VF) affects the heart’s lower chambers; AF affects the upper chambers. In AF the P-wave is nonexistent; in VF the P-wave is shown to be independent of the QRS-complex (AV-dissociation). Patients with Atrial Flutter (AFl) or AF both experience shifts in their heartbeats, but AFl causes faster heartbeats with regular RR-intervals; these are highly irregular for AF. Left Bundle Branch Block (LBBB) is a slower left ventricle, shown by irregular RR-intervals and missing P-waves, similar to AF. The QRS-duration, T_{QRS} , is >120 ms for LBBB; it is <120 ms for AF.

4.2 QRS-complex

The QRS-complex is the main element of a heartbeat in the ECG signals and will function as the guideline for the detection of the P-waves of the heartbeat. We implement a NeuroKit method that uses local maxima to detect the R-peaks of each heartbeat [42, 43].

We compute the heart rate, RR_i , at heartbeat i as the distance between consecutive peaks, and denote the difference between consecutive intervals as ΔRR_i .

$$RR_i = R_i - R_{i-1}$$

$$\Delta RR_i = |RR_i - RR_{i-1}|$$

Additional rules exclude impossible heart rhythms and wrongfully selected R-peaks. This overcomes some of the challenges caused by the remaining noise and flatlines after signal processing. Most

faulty RR-intervals come from selecting the wrong R-peak, causing too small intervals. Larger intervals can be caused by AF, but also by skipping beats and/or other diseases; since we can neither conclude nor exclude that such occurrences relate to AF, we choose to keep such intervals unaltered. According to domain experts, the RR-interval must be at least 400 ms. For smaller intervals, we compute the distance between both peaks and their previous or consecutive peak. We assume that the peak with the shortest distance is the faulty peak, and we remove it.

The Q- and S-peaks in the QRS-complex are necessary to identify the start and end of the QRS-complex, and the distance between a P-wave and its following QRS-complex. We incorporate an algorithm from NeuroKit based on the theory of a Wavelet-based ECG delineator [42, 43]. It does not select the Q- and S-peak of the first and the last QRS-complex in a recording. However, many heartbeats are included in each recording, making it sufficient to exclude these two heartbeats.

4.3 P-waves and F-waves

We limit the segment of one entire heartbeat to the interval between the end of the QRS-complex, S-peak, and the start of the next QRS-complex, Q-peak (SQ-interval). We check the validity of said SQ-intervals using rules: the S-peak must lie before the Q-peak, the next S-peak cannot lie before the Q-peak, and the SQ-interval duration must be realistic compared to the average SQ-interval of the patient: not longer than the average RR-interval. We add denoising filters to ease the identification of the waves from the remaining noise. We apply two Gaussian WMA filters: once over ten instances with a sigma of 20, and then again over 50 instances with a sigma of 25.

With the smooth signal, it is possible to apply a local maxima search technique. The segment is scaled to the range [0, 1] using min-max scaling [25, Equation 2]. Each heartbeat is now handled similarly regardless of external factors that influence the strength and quality of the recording.

We compute the patient’s average PQ-interval using the selected R-peaks. The hospital starts measuring ECGs 20 minutes before the surgery begins, giving us a baseline of clean heartbeats of each specific patient. To identify the average PQ-interval, we take the SQ-interval in these first 20 minutes and take the last wave in the range as the P-wave. All PQ-intervals in these first 20 minutes are averaged, thereby creating an average PQ-interval which we stretch a little to create the range in which a P-wave should be found. This is possible because the PQ-interval is not affected by AF. Ultimately, binary indicators on P-wave absence follow per heartbeat: P-wave existence (0), or P-wave absence (1). Three cases are considered:

- (1) **P-wave existence (0):** A wave is detected within the PQ-range for the patient, and < 3 waves exist in the range.
- (2) **F-wave occurrences (1):** A wave is detected in the PQ-range and ≥ 3 waves exist in the range.
- (3) **P-wave absence (1):** No wave is detected in the PQ-range.

We include a minimum of three waves instead of one because in this range, other waves can exist that are regular, and replacement F-waves always occur in larger multitudes. In addition, we create a second binary list keeping track of the heartbeats showing F-waves. Of the three cases mentioned above, the P-wave absence case is also stored as (0) in this list as no F-waves occur.

465 5 Incorporation in Exceptional Model Mining

466 To characterize subgroups with exceptionally elevated or decreased
 467 risk of AF, we create several updates to the Exceptional Model
 468 Mining (EMM) [16, 35] framework (cf. Section 2.2) that allow us to
 469 analyze the ECG signals as targets. The patient characteristics are
 470 the *descriptors*, the extracted ECG features are the *targets*, and AF
 471 complications serve as *evaluators*. The *model class* is ECG morphology
 472 abnormalities in the form of phenotypes.

474 5.1 Quality Measures

475 We derive multiple quality measures to assess multiple kinds of
 476 exceptional behavior in ECGs.

478 5.1.1 *Heart Rate Variability, P-wave Absence, F-wave Presence.* First,
 479 we define some statistical functions θ based on ECG phenotypes
 480 related to the Heart Rate Variability (HRV) and P-waves extracted
 481 in Section 4.1. We implement three measures (identified in AF
 482 detection methods mentioned in Section 2) to find exceptionality
 483 in the HRV: Standard Deviation of all RR-intervals (SDRR), Root
 484 Mean Square of Successive RR-interval Differences (RMSSD) and
 485 Standard Deviation of Successive RR-interval Differences (SDSD).

$$\begin{aligned}\theta_{\text{SDRR}}(r) &= \sqrt{\frac{1}{K-2} \sum_{i=1}^{K-1} (\overline{RR}_i - \overline{RR})^2} \\ \theta_{\text{RMSSD}}(r) &= \sqrt{\frac{1}{K-3} \sum_{i=1}^{K-2} (\Delta RR_i)^2} \\ \theta_{\text{SDSD}}(r) &= \sqrt{\frac{1}{K-3} \sum_{i=1}^{K-2} (\Delta RR_i - \overline{\Delta RR})^2}\end{aligned}$$

496 Here, K is the number of heartbeats, and \overline{RR} and $\overline{\Delta RR}$ are the average
 497 RR-interval and average difference between consecutive RR-
 498 intervals, respectively; r denotes the patient. We also record the
 499 percentage of heartbeats without P-waves, denoted $\theta_P(r)$, and the
 500 percentage of heartbeats displaying F-waves, denoted $\theta_F(r)$.

502 5.1.2 *Combining HRV with P-waves or F-waves.* The arrhythmias
 503 in Table 1 can be distinguished by a combination of 1) observations
 504 on HRV, and 2) P-wave absence or F-wave presence. The interest
 505 lies in finding cases where the patient experiences high HRV while
 506 either no P-wave is present in the heartbeat or replacement F-
 507 waves occur. Due to the sequential steps of our feature extraction
 508 procedure, directly matching the RR-intervals with the P-waves
 509 and/or F-waves of the same heartbeat is a bad idea. RR-intervals
 510 induce a list of S- and Q-peaks. If unmatched, S- and/or Q-peaks are
 511 filtered until only proper SQ-intervals remain. These then in turn
 512 induce the discovery of P-waves and F-waves. This makes it trivial
 513 to match P-waves and F-waves to the correct SQ-interval duration;
 514 the link with the correct RR-interval duration may be less obvious.
 515 Hence, combining P- and/or F-wave observations with RR-intervals
 516 may mislead, and hence, the following choices for θ are computed
 517 with the SQ-interval measures in place of the RR-interval.

518 We adapt SDRR, RMSSD, and SDSD such that they seek the
 519 combination of exceptional SQ-intervals (instead of RR) and either
 520 the absence of P-waves or the presence of F-waves. This leads to
 521 six additional choices for θ .

$$\begin{aligned}\theta_{\text{SDSQ}}^*(r) &= \sqrt{\frac{1}{K-2} \sum_{i=1}^{K-1} \mathbb{1}_*(r, i) \cdot (SQ_i - \overline{SQ})^2} \\ \theta_{\text{RMSSD}}^*(r) &= \sqrt{\frac{1}{K-3} \sum_{i=1}^{K-2} \mathbb{1}_*(r, i) \cdot (\Delta SQ_i)^2} \\ \theta_{\text{SDSD}}^*(r) &= \sqrt{\frac{1}{K-3} \sum_{i=1}^{K-2} \mathbb{1}_*(r, i) \cdot (\Delta SQ_i - \overline{\Delta SQ})^2}\end{aligned}$$

523 Here, $* \in \{\text{P-wave absent, F-wave present}\}$, and $\mathbb{1}$ is the indicator
 524 function (equals 1 if its subscript clause is true for heartbeat i of
 525 patient r , equals 0 if false). Recall that both the absence of P-waves
 526 and the presence of F-waves are indicators of AF.

528 5.1.3 *Correcting for Subgroup Size and Precision.* If we let the subgroup
 529 search be guided by any of the θ s defined in the previous
 530 section, the search strategy will run towards tiny subgroups covering
 531 an insubstantially small part of the data set. This is a common
 532 problem in local pattern mining: without correction for subgroup
 533 size, tiny subgroups will dominate the result set. Several solutions to
 534 this problem exist; we incorporate the entropy (denoted $\varphi_{\text{ef}}(D)$, cf.
 535 [16, Section 3.2.1]) of the split between subgroup and complement
 536 as a factor in our quality measure. Having made this correction, the
 537 search strategy discovers substantially larger subgroups, but these
 538 now also include more negatives (patients who didn't experience
 539 AF). This is not surprising: since we look at recorded signals before
 540 AF, preceding phenotypes are more subtle. To enable finding
 541 weaker phenotypes, we incorporate precision (denoted $\varphi_{\text{pr}}(D)$, cf.
 542 [19, Section 4.3]) as a factor in our quality measure. This encourages
 543 True Positives (TP) over False Positives (FP).

545 5.1.4 *Bringing it All Together.* For any of the eleven θ s from Sections
 546 5.1.1 and 5.1.2, we can compute its average $\bar{\theta}^X$ for any subset
 547 $X \subseteq \Omega$. We derive the phenotype-related $\varphi_{\text{pheno}}(D) = \bar{\theta}^{GD} - \bar{\theta}^Q$. Finally,
 548 we create a compound QM that rewards a subgroup if it scores
 549 high on all of the phenotype, entropy, and precision components.

$$\varphi(D) = \varphi_{\text{ef}}(D) \cdot \varphi_{\text{pr}}(D) \cdot \varphi_{\text{pheno}}(D) \quad (1)$$

562 5.2 Generating Candidate Subgroups

564 We employ an existing search strategy for supervised LPM: *beam
 565 search* [16, Algorithm 1]. Candidate subgroups are generated in a
 566 level-wise, general-to-specific manner. On the first level, we loop
 567 over the descriptors, generating all sensible single conditions on
 568 single attributes. Evaluating them with φ , we keep a preset number
 569 w (the *beam width*) of the best-scoring candidates as the *level-1 beam*.
 570 We generate candidates for each subsequent level i by looping
 571 over the subgroups in the $i-1$ beam, and *refining*¹ them
 572 by conjoining additional conditions, generated by looping over the
 573 attributes; after candidate generation, the best w are kept as the
 574 *level- i beam*. Beam search terminates after a predefined maximum
 575 level d (the *search depth*); the top- k subgroups encountered along
 576 the way are reported.

577 ¹using the refinement operator η from [16, Section 4.1], parameterized with the lbcna
 578 numeric refinement strategy from [45], and augmented with the ordinal refinement
 579 operator from [53].

Table 2: The number and percentage of patients in our study group that experienced the various types of AF (groups overlap; unfortunate patients may experience AF in multiple stages).

Stages	AF Complication identified	
	Yes	No
<i>before</i>	6 (2.6%)	224
<i>during</i>	6 (2.6%)	224
<i>after</i>	75 (32.6%)	155
<i>future</i>	1 (0.4%)	229
AF in general	87 (37.8%)	143

5.3 Anti-Redundancy Methods

Any EMM search strategy runs the risk of returning a top- k of very similar, exceptional subgroups: near copies of very exceptional subgroups are likely also very exceptional. This may drown out other subgroups that are also exceptional. To tackle this problem, the EMM literature contains several anti-redundancy methods.

We remove *similarity redundancy*: identical copies of descriptions whose conjuncts appear in a different order. We also remove *generalization redundancy* through description-based selection [34, 53]: if two overlapping descriptions, e.g. “age ≤ 50 ” and “age ≤ 50 AND smokes = no”, have the same quality score, the more general description is kept.

6 Experiments

Our main experiments involve proprietary hospital data. For reproducibility purposes, we repeat the experiment on a public data set; details and results can be found in Appendix A. Source code and more material are publicly available on GitHub²; our implementation builds upon the pseudocode from [16, Algorithm 1] and the implementation from [53].

6.1 Data

The data set consists of 230 patients who have undergone cardiac surgery. In total, 186 men (80.9%) and 44 women (19.1%) are included, risking bias. However, men are more prone to heart failure, thus needing cardiac surgery, than women [17]: it is a natural consequence unlikely to affect our research. Our data set includes AF complications experienced before, during, and/or after an operation, summarized in Table 2. Postoperative AF occurs in the first four weeks after surgery [44]; any AF detected later than these four weeks is considered an unrelated consequence.

The data set includes lead II ECG recordings, Electronic Health Records (EHR), and AF complication indicators. Due to the nature of the data, each entry is assumed to be a new patient; for all practical purposes, this is close enough to the truth such that the probability becomes negligible that violations of this assumption substantially affect the results of our analysis.

After transforming the EHR with aggregation and one hot encoding, we end up with 247 medical characteristics as descriptors.

²<https://github.com/liekvandenbiggelaar/EAFM>.

Subsequent filtering based on domain expertise is undesired due to the exploratory nature of beam search.

6.2 Experimental Setup

The beam search parameters are carefully chosen to combine a wide exploration of the descriptor space while keeping results clinically relevant. The search depth $d = 3$ ensures transparency and comprehensibility of the resulting descriptions; exploring conjunctions of more descriptors would be easily computationally feasible, but the resulting subgroups would be harder to interpret and more likely to be false discoveries. The beam width $w = 50$ allows for over 25% of the descriptors to participate in the level-1 beam, and keeps many potentially interesting descriptions as long as possible; we sacrifice runtime for a wider exploration of the descriptor space. The top- k descriptions to be returned is set to $k = 15$. Finally, to stimulate generality in the evidence of exceptional behavior, we set the minimum coverage of any subgroup to 5% of $|\Omega|$.

We judge the validity and medical relevance of our discovered subgroups by evaluating the content with domain experts. We round all quality scores φ to two decimals. Under this choice, we have observed identical qualities only for subgroups covering the exact same set of patients, where it is to be expected.

6.3 Results

Table 3 displays summary statistics of the results. A good subgroup has high exceptionality of the phenotype and a high percentage of AF. All experiments find more patients with AF than without, and a high exceptionality in phenotypes. Experiments on one phenotype (# 1–5) yield an average AF rate above 70%. However, they (except for θ_F) score lower on the phenotype exceptionality than most combined phenotypes (# 6–11, except for θ_{SDS}^P and θ_{SDSD}^F): those find subgroups whose phenotype is over 2.5 times more exceptional than the population. The commonality of variations in phenotypes could cause this: as many patients have one of the variational properties, the precision factor φ_{pr} has a greater effect. Hence, Experiments 1–5 find descriptions of patients who often have AF, but not necessarily exceptional ECG phenotypes, as was the objective. Experiments 6–11 find subgroups encompassing both ECG phenotypes differing from Ω and the majority of AF patients. Some episodes of AF are likely missed due to the way ECG monitoring is currently handled. Finding these cases is part of our research objective and will improve future practice in the hospital.

The remainder of the Results section will focus on the experiments with combined phenotypes only. Although experiment 5 on F-waves seems interesting from the discussion in the previous paragraph, extracting these waves from the ECG is more an art than an exact science; manual choices will influence results. The use of only this phenotype will likely lead to biased results focusing on outlier cases. Therefore, we include this only in combination with high heart rate variability.

The full top-15 subgroups reported by beam search for each of these eleven experiments can be found in Appendix B. We have discussed and postprocessed the medically most relevant findings with medical doctors at the hospital; the remainder of this section presents the results of that discussion, involving experiments with θ_{SDSD}^P , θ_{RMMSD}^P , and θ_{SDSD}^F .

Table 3: Summary statistics of the eleven experiments: experiment number, phenotype, average $\bar{\varphi}_{\text{pheno}}$ of the top-15 subgroups, average phenotype over the full data set, phenotype exceptionality factor, and percentage of patients in the subgroups that display AF (for the full data set: 37.8%).

#	Phenotype	$\bar{\varphi}_{\text{pheno}}$	$\bar{\theta}^{\Omega}$	$\frac{\bar{\varphi}_{\text{pheno}}}{\bar{\theta}^{\Omega}}$	% AF
1	θ_{SDSD}	103.38	75.38	1.37	0.71
2	θ_{RMSSD}	141.38	93.92	1.51	0.71
3	θ_{SDRR}	113.38	81.63	1.39	0.73
4	θ_P	50.48	30.38	1.66	0.71
5	θ_F	1.88	0.54	3.48	0.70
6	θ_{SDSD}^P	490.56	183.52	2.67	0.60
7	θ_{RMSSD}^P	752.20	277.89	2.71	0.58
8	θ_{SDSQ}^P	656.41	396.64	1.65	0.57
9	θ_{SDSD}^F	410.66	134.76	3.05	0.59
10	θ_{RMSSD}^F	752.20	277.89	2.71	0.58
11	θ_{SDSQ}^F	657.03	426.43	1.54	0.58

6.3.1 Subgroups Discovered with θ_{SDSD}^P . The θ_{SDSD}^P phenotype seeks patients with varying heart rate related to the standard deviation of successive SQ-interval differences, and a high percentage of missing P-waves. The top chart in Figure 3 shows that four subgroups have a low percentage of AF and five subgroups have low phenotype exceptionality. Leaving out one content-wise uninteresting subgroup, Table 16 lists the five remaining subgroups.

All subgroups select patients with acidic blood (normal/high standard bicarbonate, low anion gap, and high chloride). Three select patients with blood clotting problems (high prothrombin time), who are likely to be assisted by the heart-lung machine. A combination of these two occurs three times. In two other situations, acidic blood is combined with patients with prediabetes (normal/high glucose).

The risk groups that emerge from this experiment are patients with: (A) acidic blood and blood clotting problems (#1, #9, #11); (B) acidic blood and assisted by the heart-lung machine (#1, #9, #11); (C) acidic blood and prediabetes (#5, #6). These results are partially supported by existing literature. Low anion gap increases the risk of AF [22], just as prediabetes [27]. Furthermore, low chloride levels increase the risk of AF, but high chloride levels, as in our subgroups, show a risk similar to regular levels [21].

6.3.2 Subgroups Discovered with θ_{RMSSD}^P . The θ_{RMSSD}^P phenotype seeks patients with varying heart rate related to the root mean square of successive RR-interval differences and a high percentage of missing P-waves. The middle chart in Figure 3 shows that five subgroups have a low percentage of AF and four subgroups have low phenotype exceptionality. Four other subgroups were already discovered with θ_{SDSD}^P . Table 16 lists the two remaining subgroups.

The one new subgroup strengthens our hypothesis from the θ_{SDSD}^P experiment, on patients combining acidic blood (high chloride) with either blood clotting problems (high prothrombin time) or heart-lung machine assistance. The other new subgroup suggests exceptionality in patients receiving antibiotics (cefazolin treatment).

The emerging risk groups are patients with: (A) blood clotting problems and antibiotics administration in the form of cefazolin (#5);

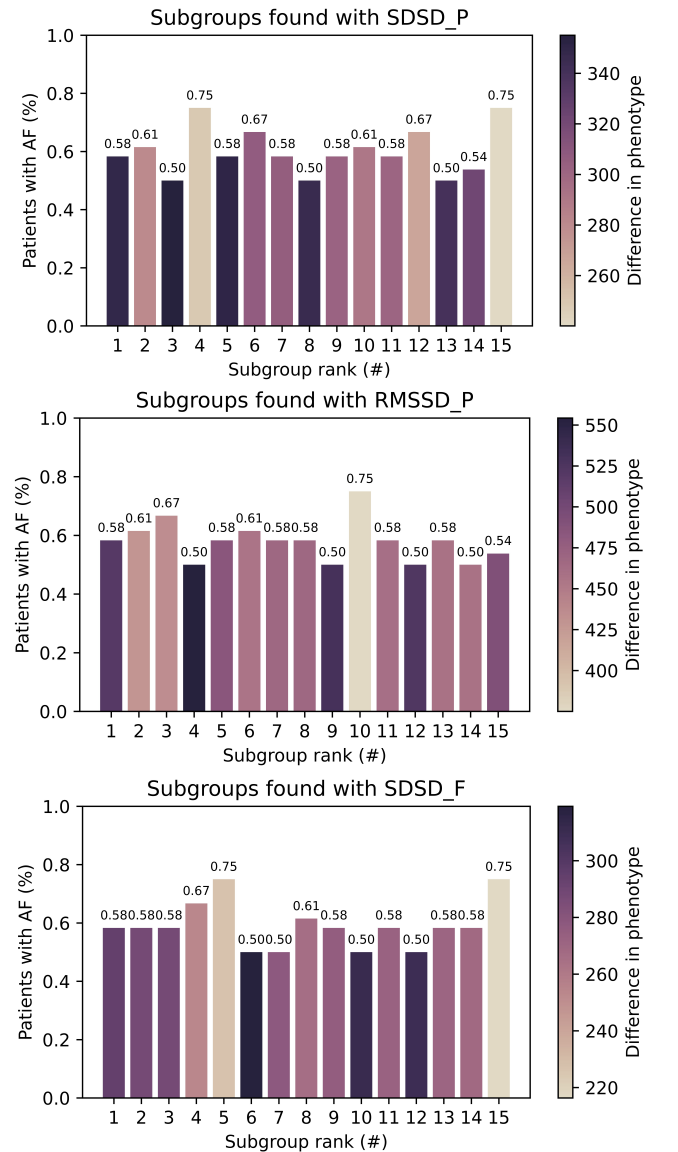


Figure 3: A visual representation of the subgroups found with the three selected experiments. The bar height shows the percentage of patients with AF, while color indicates phenotype differences from the population average.

(B) acidic blood and blood clotting problems (#13); (C) acidic blood and assisted by the heart-lung machine (#13). The administration of antibiotics has been associated with an increased risk of AF [3], but cefazolin is not yet mentioned in the list of antibiotics tested. As in the θ_{SDSD}^P experiment, high chloride is named, which contradicates results from existing literature [21].

6.3.3 Subgroups Discovered with θ_{SDSD}^F . The θ_{SDSD}^F phenotype seeks patients with varying heart rate related to standard deviation of successive SQ-interval differences and a high percentage of replacement F-waves. The bottom chart in Figure 3 shows that four

Table 4: Subgroups discovered when seeking exceptional phenotypes θ_{SDSD}^P , θ_{RMSSD}^P , and θ_{SDSD}^F . Raw values are postprocessed into qualitative statements, guided by medical professionals and medical literature.

Phenotype	#	Description
θ_{SDSD}^P	1	high prothrombin time \wedge normal/high standard bicarbonate \wedge no thrombin treatment
θ_{SDSD}^P	5	low anion gap \wedge normal/high glucose \wedge no minimally invasive aortic valve replacement
θ_{SDSD}^P	6	low anion gap \wedge normal/high glucose \wedge sex is male
θ_{SDSD}^P	9	high prothrombin time \wedge normal/high standard bicarbonate \wedge high chloride
θ_{SDSD}^P	11	high prothrombin time \wedge normal/high standard bicarbonate \wedge normal sodium
θ_{RMSSD}^P	5	high prothrombin time \wedge cefazolin treatment \wedge normal FiO_2
θ_{RMSSD}^P	13	high prothrombin time \wedge little blood loss \wedge high chloride
θ_{SDSD}^F	11	high prothrombin time \wedge Ringer's lactate treatment \wedge normal FiO_2
θ_{SDSD}^F	14	high prothrombin time \wedge normal/high standard bicarbonate \wedge normal potassium

subgroups have a low AF percentage and four have low phenotype exceptionality. Five other subgroups were already discovered with θ_{SDSD}^P or θ_{RMSSD}^P . Table 16 lists the two remaining subgroups.

Again, the overlapping subgroups complement our previous findings. One subgroup also includes patients with acidic blood (normal/high standard bicarbonate) and blood clotting problems (high prothrombin time). The remaining subgroup includes patients with blood clotting problems and a low blood volume/blood pressure (*Ringer's lactate* treatment).

The emerging risk groups are patients with: (A) blood clotting problems and low blood volume/blood pressure (#11); (B) acidic blood and blood clotting problems (#14); (C) acidic blood and assisted by the heart-lung machine (#14). Although previous research has found a higher prevalence of AF after the administration of *Ringer's lactate* [52], this treatment had not yet been associated with increased risk.

7 Conclusions

Cardiac surgery puts patients at risk of Atrial Fibrillation (AF) [44]. This heart arrhythmia is the leading cardiac cause of strokes [18]. The consequences can be avoided by preventive treatment, if we can see coming that AF is likely to occur. Current practice is reactive: medical professionals can only act when the episode is already occurring, signaled by an alarm based on unknown factors. Instead, we provide an instance of the Exceptional Model Mining (EMM) [16, 35] framework, discovering transparent and actionable subgroups of patients at a higher risk of AF. We do so by processing ECG data from patients into AF-related phenotypes, and defining quality measures that reward subgroups combining exceptional phenotype behavior, a high percentage of AF occurrence, and a substantial size. The subgroups found are hypothesized to have a higher risk of developing AF after surgery, and our advice to the hospital is to give preventive medications to patients who match the descriptions found. As we work with sensitive data, ethical considerations should be taken into account. Therefore, our research should be regarded as exploratory rather than confirming. Ideally, the knowledge derived from this paper should be confirmed in follow-up medical studies.

In that sense, the contributions of this paper are a step towards stratified medicine, where EMM automatically discovers hypotheses for interesting strata to explore further.

The method is in deployment at the Catharina Hospital in Eindhoven, the Netherlands. We conduct several experiments to select the best method for the deployment. All methods discover exceptional subgroups in terms of phenotypes and AF. Methods relying solely on heart rate variability (HRV) measurements, P-wave absence, or F-wave presence deliver subgroups with the strongest AF incidence rate. Still, the phenotypes are not that different from the overall patient population in our data set. Methods relying on combinations of on the one hand HRV and on the other hand either P-wave absence or F-wave presence, have a slightly less strong but still substantially elevated AF incidence rate, combined with strongly deviating phenotypes (cf. Table 3). Some of the subgroups we discover are defined by characteristics associated with an increased risk of AF in existing literature, thereby confirming the validity of our findings. Other subgroups we discover represent new hypotheses in this area for AF risk groups. The advice derived from the model is to administer preventive medication to prevent AF from occurring in the risk groups found and execute follow-up medical studies on the relationship of the following characteristics with the risk of AF: (1) patients assisted by the heart-lung machine that also have acidic blood; (2) patients with high chloride levels; (3) patients with blood clotting problems that need cefazolin admission to prevent infection; (4) patients with blood clotting problems that need *Ringer's lactate* to overcome low blood volume/low blood pressure.

Our experiments run on data from one of the twelve leads for measuring ECG signals. The cardiac signal preprocessing of Section 4 relies on this choice: including other leads harms the current procedure (interference, more noise), which would require more complex preprocessing steps. Since intelligently combining data from multiple leads holds the potential to provide more subtle information on the heart health of the patient, including more leads is an avenue to be explored in future work.

813
814
815
816
817
818
819
820
821
822
823
824
825
826
827
828
829
830
831
832
833
834
835
836
837
838
839
840
841
842
843
844
845
846
847
848
849
850
851
852
853
854
855
856
857
858
859
860
861
862
863
864
865
866
867
868
869
870
871
872
873
874
875
876
877
878
879
880
881
882
883
884
885
886
887
888
889
890
891
892
893
894
895
896
897
898
899
900
901
902
903
904
905
906
907
908
909
910
911
912
913
914
915
916
917
918
919
920
921
922
923
924
925
926
927
928

References

- [1] A.M.E. Abdalgawad, M.A. Hussein, H. Naeim, R. Abuelatta, and S. Alghamdy. 2019. A comparative study of TAVR versus SAVR in moderate and high-risk surgical patients: Hospital outcome and midterm results. *The Heart Surgery Forum* 22, 5 (2019), E331–E339. <https://doi.org/10.1532/hsf.2243>
- [2] S. Abhishek, S. Veni, and K.A. Narayanankutty. 2019. Biorthogonal wavelet filters for compressed sensing ECG reconstruction. *Biomedical Signal Processing and Control* 47 (2019), 183–195. <https://doi.org/10.1016/j.bspc.2018.08.011>
- [3] E. Abo-Salem, J.C. Fowler, M. Attari, C.D. Cox, A. Perez-Verdia, R. Panikkath, and K. Nugent. 2014. Antibiotic-induced cardiac arrhythmias. *Cardiovascular Therapeutics* 32, 1 (2014), 19–25. <https://doi.org/10.1111/1755-5922.12054>
- [4] R. Agrawal and S. Ramakrishnan. 1994. Fast algorithms for mining association rules in large databases. In *VLDB '94: Proceedings of the 20th International Conference on Very Large Data Bases*. VLDB, 487–499. <https://doi.org/10.5555/645920.672836>
- [5] A. Alim and M.K. Islam. 2020. Application of machine learning on ECG signal classification using morphological features. In *2020 IEEE Region 10 Symposium (TENSYMP)*. IEEE, 1632–1635. <https://doi.org/10.1109/TENSYMP50017.2020.9230780>
- [6] Z.I. Attia, P.A. Noseworthy, F. Lopez-Jimenez, S.J. Asirvatham, A.J. Deshmukh, B.J. Gersh, R.E. Carter, X. Yao, A.A. Rabinstein, B.J. Erickson, et al. 2019. An artificial intelligence-enabled ECG algorithm for the identification of patients with atrial fibrillation during sinus rhythm: A retrospective analysis of outcome prediction. *The Lancet* 394, 10201 (2019), 861–867. [https://doi.org/10.1016/S0140-6736\(19\)31721-0](https://doi.org/10.1016/S0140-6736(19)31721-0)
- [7] G. Bényász and L. Cser. 2013. Wavelet based de-noising in manufacturing and in business. *Procedia CIRP* 12 (2013), 282–287. <https://doi.org/10.1016/j.procir.2013.09.049>
- [8] G. Bianchi and R. Sorrentino. 2007. *Electronic filter simulation & design*. McGraw-Hill Education.
- [9] K.H. Boon, M. Khalil-Hani, and M.B. Malarvili. 2018. Paroxysmal atrial fibrillation prediction based on heart rate variability analysis and non-dominated sorting genetic algorithm III. *Computer Methods and Programs in Biomedicine* 153 (2018), 171–184. <https://doi.org/10.1016/j.cmpb.2017.10.012>
- [10] W. Cai, Y. Chen, J. Guo, B. Han, Y. Shi, L. Ji, J. Wang, G. Zhang, and J. Luo. 2020. Accurate detection of atrial fibrillation from 12-lead ECG using deep neural network. *Computers in Biology and Medicine* 116 (2020), 103378. <https://doi.org/10.1016/j.combiomed.2019.103378>
- [11] C.C. Chen and F.R. Tsui. 2020. Comparing different wavelet transforms on removing electrocardiogram baseline wavers and special trends. *BMC Medical Informatics and Decision Making* 20, 343 (2020). <https://doi.org/10.1186/s12911-020-01349-x>
- [12] J. Christie. 2008. One size does not fit all. *Gastrointestinal Endoscopy* 67, 2 (2008), 278–279. <https://doi.org/10.1016/j.gie.2007.10.007>
- [13] L. Clavier, J.M. Boucher, R. Lepage, J.J. Blanc, and J.C. Cornilly. 2002. Automatic P-wave analysis of patients prone to atrial fibrillation. *Medical and Biological Engineering and Computing* 40, 1 (2002), 63–71. <https://doi.org/10.1007/BF02347697>
- [14] M.B. Conover. 2003. *Understanding electrocardiography*. Elsevier Health Sciences, Chapter 1. The 12 electrocardiogram leads, 3–22.
- [15] R. Czabanski, K. Horoba, J. Wrobel, A. Matonia, R. Martinek, T. Kupka, M. Jezewski, R. Kahankova, J. Jezewski, and J.M. Leski. 2020. Detection of atrial fibrillation episodes in long-term heart rhythm signals using a support vector machine. *Sensors* 20, 3 (2020), 765. <https://doi.org/10.3390/s20030765>
- [16] W. Duivesteijn, A. Feelders, and A. Knobbe. 2016. Exceptional model mining: Supervised descriptive local pattern mining with complex target concepts. *Data Mining and Knowledge Discovery* 30 (2016), 47–98. <https://doi.org/10.1007/s10618-015-0403-4>
- [17] A. Ehdaié, E. Cingolani, M. Shehata, X. Wang, A.B. Curtis, and S.S. Chugh. 2018. Sex differences in cardiac arrhythmias: Clinical and research implications. *Circulation: Arrhythmia and Electrophysiology* 11, 3 (2018), e005680. <https://doi.org/10.1161/CIRCEP.117.005680>
- [18] K.L. Furie, L.B. Goldstein, G.W. Albers, P. Khatri, R. Neyens, M.P. Turakhia, T.N. Turan, and K.A. Wood. 2012. Oral antithrombotic agents for the prevention of stroke in nonvalvular atrial fibrillation: A science advisory for healthcare professionals from the American Heart Association/American Stroke Association. *Stroke* 43, 12 (2012), 3442–3453. <https://doi.org/10.1161/STR.0b013e318266722a>
- [19] J. Fürnkranz and P.A. Flach. 2005. Roc 'n'rule learning—towards a better understanding of covering algorithms. *Machine Learning* 58 (2005), 39–77. <https://doi.org/10.1007/s10994-005-5011-x>
- [20] D. Gamberger, N. Lavrač, A. Krstačić, and G. Krstačić. 2007. Clinical data analysis based on iterative subgroup discovery: Experiments in brain ischaemia data analysis. *Applied Intelligence* 27, 3 (2007), 205–217. <https://doi.org/10.1007/s10489-007-0068-9>
- [21] Y. Gan, S. Nie, M. Pang, R. Huang, H. Xu, B. Liu, J. Weng, C. Chunbo, H. Liu, H. Li, et al. 2024. Inverse association between serum chloride levels and the risk of atrial fibrillation in chronic kidney disease patients. *Clinical Kidney Journal* 17, 8 (2024), sfae137. <https://doi.org/10.1093/ckj/sfae137>
- [22] S. Geurts, M.J. Tilly, B. Arshi, B.H.C. Stricker, J.A. Kors, J.W. Deckers, N.M.S. de Groot, M.A. Ikram, and M. Kavousi. 2023. Heart rate variability and atrial fibrillation in the general population: A longitudinal and Mendelian randomization study. *Clinical Research in Cardiology* 112, 6 (2023), 747–758. <https://doi.org/10.1007/s00392-022-02072-5>
- [23] A.L. Goldberger, L.A.N. Amaral, L. Glass, J.M. Hausdorff, P.C. Ivanov, R.G. Mark, J.E. Mietus, G.B. Moody, C.-K. Peng, and H.E. Stanley. 2000. PhysioBank, PhysioToolkit, and PhysioNet: Components of a new research resource for complex physiologic signals. *Circulation* 101, 23 (2000), e215–e220. <https://doi.org/10.1161/01.CIR.101.23.e215>
- [24] S. Guo, X. Li, H. Liu, P. Zhang, X. Du, G. Xie, and F. Wang. 2017. Integrating temporal pattern mining in ischemic stroke prediction and treatment pathway discovery for atrial fibrillation. In *AMIA Joint Summits on Translational Science proceedings. AMIA Joint Summits on Translational Science*, Vol. 2017. AMIA, 122–130. <https://pmc.ncbi.nlm.nih.gov/articles/PMC5443383/>
- [25] H. Henderi, T. Wahyuningisih, and E. Rahwanto. 2021. Comparison of min-max normalization and Z-score normalization in the k-nearest neighbor algorithm to test the accuracy of types of breast cancer. *International Journal of Informatics and Information Systems* 4, 1 (2021), 13–20. <https://doi.org/10.47738/ijjis.v4i1.73>
- [26] K. Ishida, H. Hayashi, A. Miyamoto, Y. Sugimoto, M. Ito, Y. Murakami, and M. Horie. 2010. P wave and the development of atrial fibrillation. *Heart Rhythm* 7, 3 (2010), 289–294. <https://doi.org/10.1016/j.hrthm.2009.11.012>
- [27] C. Johansson, L. Ortendahl, M. M. Lind, J. Andersson, L. Johansson, and M. Brunström. 2023. Diabetes, prediabetes, and atrial fibrillation: A population-based cohort study based on national and regional registers. *Journal of Internal Medicine* 294, 5 (2023), 605–615. <https://doi.org/10.1111/joim.13688>
- [28] R.M. John and S. Kumar. 2016. Sinus node and atrial arrhythmias. *Circulation* 133, 19 (2016), 1892–1900. <https://doi.org/10.1161/CIRCULATIONAHA.116.018011>
- [29] S.J. Jung, C.S. Son, M.S. Kim, D.J. Kim, H.S. Park, and Y.N. Kim. 2013. Association rules to identify complications of cerebral infarction in patients with atrial fibrillation. *Healthcare Informatics Research* 19, 1 (2013), 25–32. <https://doi.org/10.4258/hir.2013.19.1.25>
- [30] R. Kher. 2019. Signal processing techniques for removing noise from ECG signals. *Journal for Biomedical Engineering* 3, 101 (2019), 1–9. <https://doi.org/10.17303/jber.2019.3.101>
- [31] W. Klösgen. 1996. Explora: A multipattern and multistrategy discovery assistant. In *Advances in Knowledge Discovery and Data Mining*. AAAI, 249–271. <https://doi.org/10.5555/257938.257965>
- [32] J. Kornej, C.S. Börschel, E.J. Benjamin, and R.B. Schnabel. 2020. Epidemiology of atrial fibrillation in the 21st century: Novel methods and new insights. *Circulation Research* 127, 1 (2020), 4–20. <https://doi.org/10.1161/CIRCRESAHA.120.316340>
- [33] J. Lee, Y. Nam, D.D. McManus, and K.H. Chon. 2013. Time-varying coherence function for atrial fibrillation detection. *IEEE Transactions on Biomedical Engineering* 60, 10 (2013), 2783–2793. <https://doi.org/10.1109/TBME.2013.2264721>
- [34] M. van Leeuwen and A. Knobbe. 2012. Diverse subgroup set discovery. *Data Mining and Knowledge Discovery* 25 (2012), 208–242. <https://doi.org/10.1007/s10618-012-0273-y>
- [35] D. Leman, A. Feelders, and A. Knobbe. 2008. Exceptional model mining. In *Machine Learning and Knowledge Discovery in Databases*, Walter Daelemans, Bart Goethals, and Katharina Morik (Eds.). Springer, Berlin, Heidelberg, 1–16. https://doi.org/10.1007/978-3-540-87481-2_1
- [36] H. Li and P. Boulauger. 2021. An automatic method to reduce baseline wander and motion artifacts on ambulatory electrocardiogram signals. *Sensors* 21, 24 (2021), 8169. <https://doi.org/10.3390/s2124169>
- [37] J. Li, M. Gao, M. Zhang, D. Liu, Z. Li, J. Du, and Y. Hou. 2020. Treatment of atrial fibrillation: A comprehensive review and practice guide. *Cardiovascular Journal of Africa* 31, 3 (2020), 153–158. <https://doi.org/10.5830/CVJA-2019-064>
- [38] Q. Li, Y. Zhang, H. Kang, Y. Xin, and C. Shi. 2017. Mining association rules between stroke risk factors based on the Apriori algorithm. *Technology and Health Care: Official Journal of the European Society for Engineering and Medicine* 25, S1 (2017), 197–205. <https://doi.org/10.3233/THC-171322>
- [39] X. Li, H. Liu, X. Du, G. Hu, G. Xie, and P. Zhang. 2016. Using frequent item set mining and feature selection methods to identify interacted risk factors: The atrial fibrillation case study. In *Studies in Health Technology and Informatics*. Vol. 228. IOS Press, 562–566. <https://doi.org/10.3233/978-1-61499-678-1-562>
- [40] L.A. Lopes and D.K. Agrawal. 2022. Post-operative atrial fibrillation: Current treatments and etiologies for a persistent surgical complication. *Journal of Surgery and Research* 5, 1 (2022), 159–172. <https://doi.org/0.26502/jsr.10020209>
- [41] E.J.S. Luz, W.B. Schwartz, G. Cámará-Chávez, and D. Menotti. 2016. ECG-based heartbeat classification for arrhythmia detection: A survey. *Computer Methods and Programs in Biomedicine* 127 (2016), 144–164. <https://doi.org/10.1016/j.cmpb.2015.12.008>
- [42] D. Makowski, T. Pham, Z.J. Lau, J.C. Brammer, F. Lespinasse, H. Pham, C. Schölzel, and A.S.H. Chen. 2021. NeuroKit2: A Python toolbox for neurophysiological signal processing. *Behavior Research Methods* 53 (2021), 1689–1696. <https://doi.org/10.3758/s13428-020-01516-y>
- [43] J.P. Martinez, R. Almeida, S. Olmos, A.P. Rocha, and P. Laguna. 2004. A wavelet-based ECG delineator: Evaluation on standard databases. *IEEE Transactions on*

- 1045 *Biomedical Engineering* 51, 4 (2004), 570–581. <https://doi.org/10.1109/TBME.2003.821031>
- 1046 [44] W.F. McIntyre. 2023. Post-operative atrial fibrillation after cardiac surgery: Challenges throughout the patient journey. *Frontiers in Cardiovascular Medicine* 10 (2023), 1156626. <https://doi.org/10.3389/fcvm.2023.1156626>
- 1047 [45] M. Meeng and A.J. Knobbe. 2021. For real: A thorough look at numeric attributes in subgroup discovery. *Data Mining and Knowledge Discovery* 35, 1 (2021), 158–212. <https://doi.org/10.1007/s10618-020-00703-x>
- 1048 [46] K. Morik, J.F. Boulicaut, and A. Siebes. 2005. *Local pattern detection*. Springer, Berlin, Heidelberg. <https://doi.org/10.1007/b137601>
- 1049 [47] H. Ogawa, Y. An, H. Nishi, S. Fukuda, K. Ishigami, S. Ikeda, K. Doi, Y. Ide, Y. Hamatani, A. Fujino, et al. 2021. Characteristics and clinical outcomes in atrial fibrillation patients classified using cluster analysis: The Fushimi atrial fibrillation registry. *EP Europace* 23, 9 (2021), 1369–1379. <https://doi.org/10.1093/europace/euab079>
- 1050 [48] J. Oster and G.D. Clifford. 2015. Impact of the presence of noise on RR interval-based atrial fibrillation detection. *Journal of Electrocardiology* 48, 6 (2015), 947–951. <https://doi.org/10.1016/j.jelectrocard.2015.08.013>
- 1051 [49] V. Pandey and V.K. Giri. 2016. High frequency noise removal from ECG using moving average filters. In *2016 International Conference on Emerging Trends in Electrical Electronics & Sustainable Energy Systems (ICETEESES)*. IEEE, 191–195. <https://doi.org/10.1109/ICETEESES.2016.7581383>
- 1052 [50] A. Parsi, M. Glavin, E. Jones, and D. Byrne. 2021. Prediction of paroxysmal atrial fibrillation using new heart rate variability features. *Computers in Biology and Medicine* 133 (2021), 104367. <https://doi.org/10.1016/j.combiomed.2021.104367>
- 1053 [51] S. Petrucci, J. Ng, G.M. Nijm, H. Al-Angari, S. Swiryn, and A.V. Sahakian. 2006. Atrial fibrillation and waveform characterization: A time domain perspective in the surface ECG. *IEEE engineering in medicine and biology magazine : the quarterly magazine of the Engineering in Medicine & Biology Society* 25, 6 (2006), 24–30. <https://doi.org/10.1109/emb-m.2006.250505>
- 1054 [52] S. Redant, Y. Langman, D. De Bels, R. Attou, and P.M. Honore. 2019. Mechanism of arrhythmias during the infusion of Ringer's acetate and Ringer's lactate solutions during cardiac surgery: New insights. *Critical Care* 23, 1 (2019), 413. <https://doi.org/10.1186/s13054-019-2696-y>
- 1055 [53] R.M. Schouten, W. Duivesteijn, and M. Pechenizkiy. 2022. Exceptional model mining for repeated cross-sectional data (EMM-RCS). In *Proceedings of the 2022 SIAM International Conference on Data Mining (SDM)*. SIAM, 585–593. <https://doi.org/10.1137/1.9781611977172.66>
- 1056 [54] K. Tateno and L. Glass. 2000. A method for detection of atrial fibrillation using RR intervals. In *Computers in Cardiology*, Vol. 27. IEEE, 391–394. <https://doi.org/10.1109/CIC.2000.89539>
- 1057 [55] M.R. Trusheim, E.R. Berndt, and F.L. Douglas. 2007. Stratified medicine: Strategic and economic implications of combining drugs and clinical biomarkers. *Nature Reviews Drug Discovery* 6, 4 (2007), 287–293. <https://doi.org/10.1038/nrd2251>
- 1058 [56] M. Vitolo, M. Proietti, A. Shantsila, G. Borhani, and G.Y.H. Lip. 2021. Clinical phenotype classification of atrial fibrillation patients using cluster analysis and associations with trial-adjudicated outcomes. *Biomedicines* 9, 7 (2021), 843. <https://doi.org/10.3390/biomedicines9070843>
- 1059 [57] X. Wang, C. Ma, Z. Zhang, H. Gao, G. Clifford, and C. Liu. 2021. Paroxysmal atrial fibrillation events detection from dynamic ECG recordings: The 4th China Physiological Signal Challenge 2021. data retrieved from Physionet, <https://physionet.org/content/cpsc2021/1.0.0/>.
- 1060 [58] S. Wrobel. 1997. An algorithm for multi-relational discovery of subgroups. In *Principles of Data Mining and Knowledge Discovery, First European Symposium, PKDD '97, Trondheim, Norway, June 24–27, 1997, Proceedings (Lecture Notes in Computer Science, Vol. 1263)*. Springer, Berlin, Heidelberg, 78–87. https://doi.org/10.1007/3-540-63223-9_108
- 1061 [59] Y. Xia, N. Wulan, K. Wang, and H. Zhang. 2018. Detecting atrial fibrillation by deep convolutional neural networks. *Computers in Biology and Medicine* 93 (2018), 84–92. <https://doi.org/10.1016/j.combiomed.2017.12.007>

A Experiment on Publicly Available Data

As mentioned in Section 6, the experiments in the paper are carried out on hospital data that is not available for public distribution. We repeat the experiments on a synthetic data set to allow reproduction.

A.1 Synthetic Data

The data in this experiment combines synthetic and public data: synthetically generated Electronic Health Records (EHR), Electrocardiogram (ECG) signals from the CPSC 2021 database [23, 57], and corresponding Atrial Fibrillation (AF) indicators from the matching the signals from the database.

Table 5: Top-1 subgroups discovered when seeking all eleven exceptional phenotypes on the publicly available data.

Phenotype	Description	φ	% AF
θ_{SDSD}	Using a6 \wedge a13 \in [1172; 1816]	1.94	85.7
θ_{RMSSD}	Using a6 \wedge a13 \in [1172; 1816]	3.02	85.7
θ_{SDRR}	a14 \in [881; 2332] \wedge a54 is not taken \wedge a38 is not taken	1.72	83.3
θ_P	a46 is taken \wedge a10 \in [0; 0] \wedge a11 \in [0; 273]	1.73	100.0
θ_F	a43 is taken \wedge a3 is underweight	0.14	80.0
θ_{SDSD}^P	a48 is taken \wedge a2 is male \wedge a9 \in [221; 2256]	2.58	87.5
θ_{RMSSD}^P	a43 taken \wedge a12 \in [84; 2463] \wedge a34 is not taken	12.26	80.0
θ_{SDSQ}^P	a43 taken \wedge a13 \in [0; 0] \wedge a47 is not taken	8.88	80.0
θ_{SDSD}^F	a48 taken \wedge a2 is male \wedge a9 \in [221; 2256]	2.82	87.5
θ_{RMSSD}^F	a43 taken \wedge a12 \in [84; 2463] \wedge a34 is not taken	12.26	80.0
θ_{SDSQ}^F	a43 is taken \wedge a38 is not taken \wedge a47 is not taken	3.08	83.3

A.1.1 Electronic Health Records. The EHR characteristics function as the descriptors (a_1, \dots, a_M) of the Exceptional Model Mining (EMM) framework. We produce 57 realistic medical attributes, renamed to **a1**, **a2**, ... because of the sensitive nature of medical data. This process is performed at random while maintaining medical patterns. (**a1**, ..., **a4**) concern information, where the age is selected between 50 and 80 years, the sex is skewed towards men (this follows the trend in hospital data that more men get cardiac surgery [17]), the BMI is skewed towards healthy and slightly overweight patients, and the ASA score is randomly selected between 1 and 6, getting progressively worse. (**a5**, ..., **a7**) contains information about habits that randomly pick one of the options {None, Used, Uses}. (**a8**, ..., **a14**) has information on fluid loss during cardiac surgery, which has a 60% chance of being 0, and a 40% chance of being randomly sampled between 0 and 2500. Lastly, (**a15**, ..., **a57**) are medications that patients can take at home, the options are {Not taken, Taken} and they are sampled in an 80/20 ratio. Each combination of medical characteristics belongs to one patient.

A.1.2 Electrocardiogram Signals. The ECG signals form the basis for our targets (ℓ_1, \dots, ℓ_K). These targets are extracted from the ECG signals in the CPSC 2021 data set. It includes ECG signals from 105 patients with (49) and without (56) AF. The signals are stored in segments per patient and were originally divided into training sets I and II. However, we combined all of them into one data set. As the quantity of data segments was too large, it became infeasible

1103
1104
1105
1106
1107
1108
1109
1110
1111
1112
1113
1114
1115
1116
1117
1118
1119
1120
1121
1122
1123
1124
1125
1126
1127
1128
1129
1130
1131
1132
1133
1134
1135
1136
1137
1138
1139
1140
1141
1142
1143
1144
1145
1146
1147
1148
1149
1150
1151
1152
1153
1154
1155
1156
1157
1158
1159
1160

1161 to combine all segments to obtain an ECG per patient. Thus, we
 1162 denoise and extract the features per segment, and concatenate the
 1163 extracted features so that the final data set has one row per patient.
 1164 One main difference between the private hospital data and this
 1165 public data set is the sampling frequency, which is 500 Hz and 200
 1166 Hz respectively. The effect on denoising is negligible, but the R-peak
 1167 correction is altered to fit the frequency. The extra denoising on
 1168 the SQ-interval that originally contained two weighted average
 1169 filters now only includes the first one ($\sigma = 20, M = 10$) to prevent
 1170 over-smoothing (cf. Section 5). Ultimately, we successfully extract
 1171 the ECG features of 97 of the 105 patients.

1172 **A.1.3 Atrial Fibrillation Indicators.** A binary indicator (b_1) func-
 1173 tions as the *evaluator*. These labels in the ECG data set indicate
 1174 whether the patient does or does not experience AF in the recording.
 1175

1176

1177

1178

1179

1180

1181

1182

1183

1184

1185

1186

1187

1188

1189

1190

1191

1192

1193

1194

1195

1196

1197

1198

1199

1200

1201

1202

1203

1204

1205

1206

1207

1208

1209

1210

1211

1212

1213

1214

1215

1216

1217

1218

A.2 Results

1219 For each of the eleven experiments, we deploy Exceptional Model
 1220 Mining (EMM) on the descriptors and targets. One description is
 1221 generated per experiment and described in Table 5. These descrip-
 1222 tions do not contain sensitive information, as their sole purpose is
 1223 reproducibility. The processed data is available in the repository
 1224 but can also be processed again. However, keep in mind that this
 1225 takes over two hours. When deployed, a new ECG instance can
 1226 be easily added to the processed list of quality measures and AF
 1227 complications. Adding this takes about five minutes maximum. The
 1228 beam search on these processed lists takes only 15 seconds.
 1229

B Additional Results on Hospital Data

1230 The following pages contain information on the subgroups in each
 1231 of the eleven experiments.
 1232

1233

1234

1235

1236

1237

1238

1239

1240

1241

1242

1243

1244

1245

1246

1247

1248

1249

1250

1251

1252

1253

1254

1255

1256

1257

1258

1259

1260

1261

1262

1263

1264

1265

1266

1267

1268

1269

1270

1271

1272

1273

1274

1275

Table 6: Top-15 subgroups discovered when seeking exceptional phenotype θ_{SDSD} .

Phenotype	#	Description
θ_{SDSD}	1	anion gap venous $\in (0.0; 3.0)$ \wedge age $\in (70; 88)$ \wedge fluid loss $\in (0.0; 0.0)$
θ_{SDSD}	2	age $\in (71; 88)$ \wedge anion gap venous $\in (0.0; 3.0)$ \wedge fluid loss $\in (0.0; 0.0)$
θ_{SDSD}	3	age $\in (71; 88)$ \wedge Euroscore-I $\in (5.7; 40.7)$ \wedge potassium $\in (3.9; 5.1)$
θ_{SDSD}	4	glucose (arterial) $\in (4.0; 6.0)$ \wedge blood loss $\in (641.6; 3868.0)$ \wedge Midazolam-hameln 5 mg/ml IV administration $\in (0.0; 0.0)$
θ_{SDSD}	5	Euroscore-I $\in (6.4; 85.7)$ \wedge age $\in (71; 88)$ \wedge potassium $\in (4.1; 5.1)$
θ_{SDSD}	6	glucose (arterial) $\in (4.0; 6.0)$ \wedge blood loss $\in (641.6; 3868.0)$ \wedge anion gap $\in (0.0; 6.0)$
θ_{SDSD}	7	anion gap venous $\in (0.0; 3.0)$ \wedge age $\in (70; 88)$ \wedge lactate $\in (1.3; 2.8)$
θ_{SDSD}	8	age $\in (71; 88)$ \wedge anion gap venous $\in (0.0; 3.0)$ \wedge lactate $\in (1.3; 2.8)$
θ_{SDSD}	9	anion gap venous $\in (0.0; 3.0)$ \wedge age $\in (70; 88)$ \wedge fluid loss $\in (0.0; 9.6)$
θ_{SDSD}	10	age $\in (71; 88)$ \wedge anion gap venous $\in (0.0; 3.0)$ \wedge fluid loss $\in (0.0; 9.6)$
θ_{SDSD}	11	anion gap venous $\in (0.0; 3.0)$ \wedge age $\in (73; 88)$ \wedge lactate $\in (1.3; 2.8)$
θ_{SDSD}	12	age $\in (75; 88)$ \wedge protamin administration $\in (14.3; 21.1)$ \wedge PCO2 $\in (37.0; 45.2)$
θ_{SDSD}	13	glucose arterial $\in (4.0; 6.0)$ \wedge blood loss $\in (641.6; 3868.0)$ \wedge SO2 $\in (77.8; 100.0)$
θ_{SDSD}	14	Euroscore-I $\in (2.4; 85.7)$ \wedge taking pantoprazole = True \wedge priority $\in \{\text{unknown, plannable, } < 1 \text{ week}\}$
θ_{SDSD}	15	Euroscore-I $\in (2.4; 85.7)$ \wedge taking pantoprazole = True \wedge priority $\in \{\text{unknown, plannable, } < 1 \text{ week, } < 72 \text{ hours}\}$

Table 7: Top-15 subgroups discovered when seeking exceptional phenotype θ_{RMSSD} .

Phenotype	#	Description	
θ_{RMSSD}	1	anion gap venous $\in (0.0; 3.0)$ \wedge age $\in (70; 88)$ \wedge fluid loss $\in (0.0; 0.0)$	1362
θ_{RMSSD}	2	age $\in (71; 88)$ \wedge anion gap venous $\in (0.0; 3.0)$ \wedge fluid loss $\in (0.0; 0.0)$	1363
θ_{RMSSD}	3	anion gap venous $\in (0.0; 3.0)$ \wedge age $\in (73; 88)$ \wedge potassium $\in (1.3; 2.8)$	1364
θ_{RMSSD}	4	anion gap venous $\in (0.0; 3.0)$ \wedge age $\in (70; 88)$ \wedge lactate $\in (1.3; 2.8)$	1365
θ_{RMSSD}	5	age $\in (71; 88)$ \wedge anion gap venous $\in (0.0; 3.0)$ \wedge lactate $\in (1.3; 2.8)$	1366
θ_{RMSSD}	6	anion gap venous $\in (0.0; 3.0)$ \wedge age $\in (70; 88)$ \wedge fluid loss $\in (0.0; 9.6)$	1367
θ_{RMSSD}	7	age $\in (71; 88)$ \wedge anion gap venous $\in (0.0; 3.0)$ \wedge fluid loss $\in (0.0; 9.6)$	1368
θ_{RMSSD}	8	glucose (arterial) $\in (4.0; 6.0)$ \wedge blood loss $\in (641.6; 3868.0)$ \wedge thrombocytes $\in (99.0; 170.0)$	1369
θ_{RMSSD}	9	glucose (arterial) $\in (4.0; 6.0)$ \wedge blood loss $\in (641.6; 3868.0)$ \wedge anion gap $\in (0.0; 6.0)$	1370
θ_{RMSSD}	10	anion gap venous $\in (0.0; 3.0)$ \wedge alfentanil administration $\in (3.0; 21.3)$ \wedge taking atorvastatin = False	1371
θ_{RMSSD}	11	anion gap venous $\in (0.0; 3.0)$ \wedge alfentanil administration $\in (3.0; 21.3)$	1372
θ_{RMSSD}	12	milrinone administration $\in (3.5; 635.4)$ \wedge phenylephrine administration $\in (0.0; 9.4)$ \wedge fibrinogen $\in (2.1; 4.4)$	1373
θ_{RMSSD}	13	glucose (arterial) $\in (4.0; 6.0)$ \wedge blood loss $\in (641.6; 3868.0)$ \wedge Midazolam-hameln 5 mg/ml IV administration $\in (0.0; 0.0)$	1374
θ_{RMSSD}	14	anion gap venous $\in (0.0; 3.0)$ \wedge age $\in (73; 88)$ \wedge fluid loss $\in (0.0; 10.0)$	1375
θ_{RMSSD}	15	age $\in (75; 88)$ \wedge Euroscore-I $\in (2.4; 85.7)$ \wedge priority $\in \{\text{unknown, plannable, } < 1 \text{ week, } < 72 \text{ hours}\}$	1376

Table 8: Top-15 subgroups discovered when seeking exceptional phenotype θ_{SDRR} .

1393	1451	
1394	1452	
1395	1453	
1396	1454	
1397	1455	
1398	1456	
1399	1457	
1400	1458	
1401	1459	
1402	1460	
1403	1461	
1404	1462	
1405	1463	
1406	1464	
1407	1465	
1408	1466	
1409	1467	
1410	1468	
1411	1469	
1412	1470	
1413	1471	
1414	1472	
1415	1473	
1416	1474	
1417	1475	
1418	1476	
1419	1477	
1420	1478	
1421	1479	
Phenotype	#	Description
θ_{SDRR}	1	age $\in (71; 88) \wedge$ taking acetylsalicylic acid = True \wedge morphine administration $\in (0.0; 0.9)$
θ_{SDRR}	2	anion gap venous $\in (0.0; 3.0) \wedge$ age $\in (70; 88) \wedge$ fluid loss $\in (0.0; 0.0)$
θ_{SDRR}	3	age $\in (71; 88) \wedge$ anion gap venous $\in (0.0; 3.0) \wedge$ fluid loss $\in (0.0; 0.0)$
θ_{SDRR}	4	anion gap venous $\in (0.0; 3.0) \wedge$ APTTCkprest = unknown \wedge hemoglobin $\in (3.7; 6.5)$
θ_{SDRR}	5	age $\in (71; 88) \wedge$ bicarbonate $\in (19.0; 23.6) \wedge$ NovoRapid administration $\in (0.0; 0.0)$
θ_{SDRR}	6	glucose $\in (4.1; 6.0) \wedge$ blood loss $\in (570.4; 3868.0) \wedge$ Midazolam-hameln 5 mg/ml IV administration $\in (0.0; 0.0)$
θ_{SDRR}	7	glucose (arterial) $\in (4.0; 6.0) \wedge$ blood loss $\in (641.6; 3868.0) \wedge$ SO2 $\in (77.8; 100.0)$
θ_{SDRR}	8	anion gap venous $\in (0.0; 3.0) \wedge$ age $\in (70; 88) \wedge$ fluid loss $\in (0.0; 9.6)$
θ_{SDRR}	9	age $\in (71; 88) \wedge$ anion gap venous $\in (0.0; 3.0) \wedge$ fluid loss $\in (0.0; 9.6)$
θ_{SDRR}	10	glucose (arterial) $\in (4.0; 6.0) \wedge$ alfentanil administration $\in (29.4; 54.6) \wedge$ calcium gluconate administration $\in (20.0; 70.0)$
θ_{SDRR}	11	anion gap venous $\in (0.0; 3.0) \wedge$ APTTCkprest = unknown \wedge carboxyhemoglobin $\in (1.2; 1.8)$
θ_{SDRR}	12	age $\in (71; 88) \wedge$ bicarbonate $\in (19.0; 23.6) \wedge$ Midazolam-hameln 5 mg/ml IV administration $\in (0.0; 0.0)$
θ_{SDRR}	13	age $\in (75; 88) \wedge$ bicarbonate $\in (19.6; 25.6) \wedge$ smoking $\in \{\text{never done, done in the past}\}$
θ_{SDRR}	14	anion gap venous $\in (0.0; 3.0) \wedge$ age $\in (70; 88) \wedge$ lactate $\in (1.3; 2.8)$
θ_{SDRR}	15	age $\in (71; 88) \wedge$ anion gap venous $\in (0.0; 3.0) \wedge$ lactate $\in (1.3; 2.8)$

Table 9: Top-15 subgroups discovered when seeking exceptional phenotype θ_P .

1418	1476	
1419	1477	
1420	1478	
1421	1479	
Phenotype	#	Description
θ_P	1	sodium $\in (112.0; 135.0) \wedge$ taking metoprolol = True \wedge fluid loss $\in (0.0; 24.0)$
θ_P	2	sodium $\in (112.0; 135.0) \wedge$ taking metoprolol = True \wedge fluid loss $\in (0.0; 0.0)$
θ_P	3	sodium $\in (112.0; 135.0) \wedge$ taking metoprolol = True \wedge coronary artery bypass grafting = False
θ_P	4	creatinine $\in (48.0; 73.6) \wedge$ PO2 $\in (38.0; 230.0) \wedge$ dexamethasone administration $\in (0.0; 4.1)$
θ_P	5	Euroscore-I $\in (2.4; 85.7) \wedge$ CK $\in (303.0; 841.0) \wedge$ phenylephrine administration $\in (0.0; 3.5)$
θ_P	6	Euroscore-I $\in (2.4; 85.7) \wedge$ CK $\in (303.0; 841.0) \wedge$ methemoglobin $\in (0.7; 1.9)$
θ_P	7	cardioplegia $\in (1078.4; 4629.0) \wedge$ base excess $\in (-1.3; 3.4) \wedge$ glucose $\in (5.2; 7.7)$
θ_P	8	hemoglobin $\in (3.7; 5.8) \wedge$ eGFR (CKD-EPI) $\in (62.4; 91.0) \wedge$ anion gap $\in (0.0; 4.0)$
θ_P	9	hemoglobin $\in (3.7; 5.8) \wedge$ eGFR (CKD-EPI) $\in (62.4; 91.0) \wedge$ carboxyhemoglobin $\in (0.9; 1.8)$
θ_P	10	taking pantoprazole = True \wedge thrombocytes $\in (120.0; 244.0) \wedge$ morphine administration $\in (0.0; 0.9)$
θ_P	11	hemoglobin $\in (3.7; 5.8) \wedge$ creatinine $\in (62.0; 98.0) \wedge$ age $\in (54; 73)$
θ_P	12	Euroscore-I $\in (2.4; 85.7) \wedge$ CK $\in (303.0; 841.0) \wedge$ methemoglobin $\in (0.8; 1.9)$
θ_P	13	CK $\in (362.2; 1723.0) \wedge$ Euroscore-I $\in (1.6; 16.6) \wedge$ glucose $\in (6.2; 11.4)$
θ_P	14	CK $\in (362.2; 1723.0) \wedge$ Euroscore-I $\in (1.6; 16.6) \wedge$ age $\in (61; 73)$
θ_P	15	cardioplegia $\in (1078.4; 4629.0) \wedge$ base excess $\in (-1.3; 3.4) \wedge$ morphine administration $\in (0.0; 0.8)$

Table 10: Top-15 subgroups discovered when seeking exceptional phenotype θ_P .

Phenotype	#	Description
θ_F	1	hematocrit $\in (0.2; 0.3)$ \wedge glucose $\in (8.2; 12.7)$ \wedge drug usage $\in \{\text{never used, used in the past}\}$
θ_F	2	hematocrit $\in (0.2; 0.3)$ \wedge glucose $\in (8.2; 12.7)$ \wedge drug usage $\in \{\text{never used}\}$
θ_F	3	hematocrit $\in (0.2; 0.3)$ \wedge glucose $\in (8.2; 12.7)$ \wedge albumin administration $\in (0.0; 0.0)$
θ_F	4	hematocrit $\in (0.2; 0.3)$ \wedge glucose $\in (8.2; 12.7)$ \wedge modified gelatin administration $\in (0.0; 0.0)$
θ_F	5	neutrophils $\in (6.8; 23.0)$ \wedge CK $\in (91.0; 554.8)$ \wedge morphine administration $\in (0.2; 2.8)$
θ_F	6	neutrophils $\in (6.8; 23.0)$ \wedge morphine administration $\in (0.2; 2.8)$ \wedge PO2 $\in (38.0; 196.4)$
θ_F	7	neutrophils $\in (6.8; 23.0)$ \wedge CK $\in (91.0; 554.8)$ \wedge cell salvage administration $\in (0.0; 1318.3)$
θ_F	8	neutrophils $\in (6.8; 23.0)$ \wedge PO2 $\in (36.0; 194.2)$ \wedge clonidine administration $\in (0.0; 0.0)$
θ_F	9	eosinophils $\in (-1.0; -1.0)$ \wedge potassium $\in (4.2; 5.8)$ \wedge PO2 $\in (38.0; 192.0)$
θ_F	10	APTT (heparanase) $\in (27.4; 46.5)$ \wedge hematocrit $\in (0.24; 0.33)$ \wedge BMI $\in \{\text{underweight, healthy, overweight, obese}\}$
θ_F	11	leucocytes $\in (8.1; 57.6)$ \wedge monocytes $\in (0.2; 0.8)$ \wedge taking losartan with diuretics = False
θ_F	12	APTT (heparanase) $\in (27.4; 46.5)$ \wedge hematocrit $\in (0.2; 0.3)$ \wedge pH $\in (7.3; 7.4)$
θ_F	13	hematocrit $\in (0.2; 0.3)$ \wedge rocuronium administration $\in (0.0; 0.0)$ \wedge priority $\in \{\text{unknown, plannable, < 1 week, < 72 hours}\}$
θ_F	14	neutrophils $\in (6.8; 23.0)$ \wedge CK $\in (91.0; 554.8)$ \wedge thrombocytes $\in (67.0; 232.0)$
θ_F	15	neutrophils $\in (6.8; 23.0)$ \wedge morphine administration $\in (0.2; 2.8)$ \wedge potassium $\in (3.8; 5.8)$

Table 11: Top-15 subgroups discovered when seeking exceptional phenotype θ_{SPSP}^P .

Phenotype	#	Description
θ_{SDSD}^P	1	prothrombin time $\in (16.5; 131.0)$ \wedge standard bicarbonate $\in (23.7; 27.3)$ \wedge thrombin administration $\in (0.0; 0.0)$
θ_{SDSD}^P	2	fibrinogen $\in (1.7; 7.7)$ \wedge base excess $\in (-0.6; 7.3)$ \wedge thrombin administration $\in (0.0; 0.0)$
θ_{SDSD}^P	3	prothrombin time $\in (17.7; 131.0)$ \wedge base excess $\in (-0.6; 3.2)$ \wedge calcium ions $\in (1.1; 1.2)$
θ_{SDSD}^P	4	milrinone administration $\in (3.5; 635.4)$ \wedge dexamethasone administration $\in (0.0; 2.6)$ \wedge chloride $\in (97.0; 111.0)$
θ_{SDSD}^P	5	anion gap $\in (-1.0; 2.0)$ \wedge glucose (arterial) $\in (4.7; 6.7)$ \wedge minimally invasive aortic valve replacement = False
θ_{SDSD}^P	6	anion gap $\in (-1.0; 2.0)$ \wedge glucose $\in (4.1; 6.7)$ \wedge sex = male
θ_{SDSD}^P	7	prothrombin time $\in (17.7; 131.0)$ \wedge noradrenalin administration $\in (0.0; 24.6)$ \wedge fluid loss $\in (0.0; 0.0)$
θ_{SDSD}^P	8	prothrombin time $\in (17.7; 131.0)$ \wedge blood loss $\in (0.0; 958.8)$ \wedge age $\in (51; 74)$
θ_{SDSD}^P	9	prothrombin time $\in (16.5; 131.0)$ \wedge standard bicarbonate $\in (23.7; 27.3)$ \wedge chloride $\in (105.0; 110.0)$
θ_{SDSD}^P	10	prothrombin time $\in (17.7; 131.0)$ \wedge standard bicarbonate $\in (23.8; 27.3)$ \wedge calcium ions $\in (1.1; 1.2)$
θ_{SDSD}^P	11	prothrombin time $\in (17.7; 131.0)$ \wedge standard bicarbonate $\in (23.8; 27.3)$ \wedge sodium $\in (133.0; 141.0)$
θ_{SDSD}^P	12	prothrombin time $\in (17.7; 131.0)$ \wedge standard bicarbonate $\in (23.8; 27.3)$ \wedge alfentanil administration $\in (0.0; 42.3)$
θ_{SDSD}^P	13	prothrombin time $\in (17.7; 131.0)$ \wedge blood loss $\in (0.0; 958.8)$ \wedge fluid loss $\in (0.0; 0.0)$
θ_{SDSD}^P	14	prothrombin time $\in (16.5; 131.0)$ \wedge standard bicarbonate $\in (23.7; 27.3)$ \wedge sodium $\in (132.2; 141.0)$
θ_{SDSD}^P	15	milrinone administration $\in (3.5; 635.4)$ \wedge cefazolin administration $\in (0.0; 92.5)$ \wedge prothrombin time $\in (14.8; 131.0)$

Table 12: Top-15 subgroups discovered when seeking exceptional phenotype θ_{RMSSD}^P .

Phenotype	#	Description
θ_{RMSSD}^P	1	prothrombin time $\in (16.5; 131.0)$ \wedge standard bicarbonate $\in (23.7; 27.3)$ \wedge thrombin administration $\in (0.0; 0.0)$
θ_{RMSSD}^P	2	fibrinogen $\in (1.7; 7.7)$ \wedge base excess $\in (-0.6; 7.3)$ \wedge thrombin administration $\in (0.0; 0.0)$
θ_{RMSSD}^P	3	prothrombin time $\in (17.7; 131.0)$ \wedge standard bicarbonate $\in (23.8; 27.3)$ \wedge alfentanil administration $\in (0.0; 42.3)$
θ_{RMSSD}^P	4	prothrombin time $\in (17.7; 131.0)$ \wedge base excess $\in (-0.7; 3.2)$ \wedge calcium ions $\in (1.1; 1.2)$
θ_{RMSSD}^P	5	prothrombin time $\in (17.7; 131.0)$ \wedge cefazolin administration $\in (0.0; 90.3)$ \wedge FIO2 $\in (0.2; 0.2)$
θ_{RMSSD}^P	6	prothrombin time $\in (17.7; 131.0)$ \wedge standard bicarbonate $\in (23.8; 27.3)$ \wedge calcium ions $\in (1.1; 1.2)$
θ_{RMSSD}^P	7	prothrombin time $\in (16.5; 131.0)$ \wedge standard bicarbonate $\in (23.7; 27.3)$ \wedge chloride $\in (105.0; 110.0)$
θ_{RMSSD}^P	8	prothrombin time $\in (17.7; 131.0)$ \wedge standard bicarbonate $\in (23.8; 27.3)$ \wedge sodium $\in (133.0; 141.0)$
θ_{RMSSD}^P	9	prothrombin time $\in (17.7; 131.0)$ \wedge blood loss $\in (0.0; 958.8)$ \wedge age $\in (51; 74)$
θ_{RMSSD}^P	10	milrinone administration $\in (3.5; 635.4)$ \wedge cefazolin administration $\in (0.0; 92.5)$ \wedge prothrombin time $\in (14.8; 131.0)$
θ_{RMSSD}^P	11	prothrombin time $\in (17.7; 131.0)$ \wedge noradrenalin administration $\in (0.0; 24.6)$ \wedge fluid loss $\in (0.0; 0.0)$
θ_{RMSSD}^P	12	prothrombin time $\in (17.7; 131.0)$ \wedge blood loss $\in (0.0; 958.8)$ \wedge fluid loss $\in (0.0; 0.0)$
θ_{RMSSD}^P	13	prothrombin time $\in (17.7; 131.0)$ \wedge blood loss $\in (0.0; 958.8)$ \wedge chloride $\in (105.0; 111.0)$
θ_{RMSSD}^P	14	fibrinogen $\in (1.7; 7.7)$ \wedge standard bicarbonate $\in (23.8; 30.2)$ \wedge drains $\in (0.0; 480.0)$
θ_{RMSSD}^P	15	prothrombin time $\in (17.7; 131.0)$ \wedge base excess $\in (-0.7; 3.2)$ \wedge coronary artery bypass grafting = False

Table 13: Top-15 subgroups discovered when seeking exceptional phenotype θ_{SDSO}^P .

Phenotype	#	Description
θ_{SDSQ}^P	1	prothrombin time $\in (17.7; 131.0)$ \wedge standard bicarbonate $\in (23.8; 27.3)$ \wedge age $\in (51; 74)$
θ_{SDSQ}^P	2	prothrombin time $\in (17.7; 131.0)$ \wedge noradrenalin administration $\in (0.0; 24.6)$ \wedge fluid loss $\in (0.0; 0.0)$
θ_{SDSQ}^P	3	fibrinogen $\in (1.7; 7.7)$ \wedge base excess $\in (-0.6; 7.3)$ \wedge thrombin administration $\in (0.0; 0.0)$
θ_{SDSQ}^P	4	base excess $\in (-0.6; 7.3)$ \wedge fibrinogen $\in (2.1; 7.7)$ \wedge thrombin administration $\in (0.0; 0.0)$
θ_{SDSQ}^P	5	anion gap $\in (-1.0; 2.0)$ \wedge glucose $\in (4.1; 6.7)$ \wedge sex = male
θ_{SDSQ}^P	6	prothrombin time $\in (17.7; 131.0)$ \wedge blood loss $\in (0.0; 958.8)$ \wedge age $\in (51; 74)$
θ_{SDSQ}^P	7	prothrombin time $\in (17.7; 131.0)$ \wedge cefazolin administration $\in (0.0; 90.3)$ \wedge taking pantoprazole = False
θ_{SDSQ}^P	8	standard bicarbonate $\in (23.7; 30.2)$ \wedge alfentanil administration $\in (30.5; 55.4)$ \wedge calcium ions $\in (1.1; 1.2)$
θ_{SDSQ}^P	9	prothrombin time $\in (17.7; 131.0)$ \wedge blood loss $\in (0.0; 958.8)$ \wedge fluid loss $\in (0.0; 0.0)$
θ_{SDSQ}^P	10	base excess $\in (-0.6; 7.3)$ \wedge prothrombin time $\in (16.4; 131.0)$ \wedge alfentanil administration $\in (0.0; 46.3)$
θ_{SDSQ}^P	11	base excess $\in (-0.6; 7.3)$ \wedge prothrombin time $\in (16.4; 131.0)$ \wedge fibrinogen administration $\in (0.0; 40.0)$
θ_{SDSQ}^P	12	base excess $\in (-0.6; 7.3)$ \wedge prothrombin time $\in (16.4; 131.0)$ \wedge fibrinogen administration $\in (0.0; 0.0)$
θ_{SDSQ}^P	13	prothrombin time $\in (17.7; 131.0)$ \wedge base excess $\in (-0.7; 3.2)$ \wedge calcium ions $\in (1.1; 1.2)$
θ_{SDSQ}^P	14	glucose (arterial) $\in (4.0; 6.7)$ \wedge anion gap $\in (-1.0; 2.0)$ \wedge minimally invasive aortic valve replacement = False
θ_{SDSQ}^P	15	base excess $\in (-0.6; 7.3)$ \wedge prothrombin time $\in (16.4; 131.0)$ \wedge age $\in (51; 73)$

Table 14: Top-15 subgroups discovered when seeking exceptional phenotype θ_{SDSD}^F .

Phenotype	#	Description	
θ_{SDSD}^F	1	prothrombin time $\in (16.5; 131.0)$ \wedge standard bicarbonate $\in (23.7; 27.3)$ \wedge thrombin administration $\in (0.0; 0.0)$	1799
θ_{SDSD}^F	2	prothrombin time $\in (17.7; 131.0)$ \wedge cefazolin administration $\in (0.0; 90.3)$ \wedge FIO2 $\in (0.2; 0.2)$	1800
θ_{SDSD}^F	3	prothrombin time $\in (17.7; 131.0)$ \wedge noradrenalin administration $\in (0.0; 24.6)$ \wedge fluid loss $\in (0.0; 0.0)$	1801
θ_{SDSD}^F	4	prothrombin time $\in (17.7; 131.0)$ \wedge standard bicarbonate $\in (23.8; 27.3)$ \wedge alfentanil administration $\in (0.0; 42.3)$	1802
θ_{SDSD}^F	5	milrinone administration $\in (3.5; 635.4)$ \wedge cefazolin administration $\in (0.0; 92.5)$ \wedge prothrombin time $\in (14.8; 131.0)$	1803
θ_{SDSD}^F	6	prothrombin time $\in (17.7; 131.0)$ \wedge base excess $\in (-0.7; 3.2)$ \wedge calcium ions $\in (1.1; 1.2)$	1804
θ_{SDSD}^F	7	fibrinogen $\in (1.7; 7.7)$ \wedge standard bicarbonate $\in (23.8; 30.2)$ \wedge drains $\in (0.0; 480.0)$	1805
θ_{SDSD}^F	8	prothrombin time $\in (17.7; 131.0)$ \wedge standard bicarbonate $\in (23.8; 27.3)$ \wedge calcium ions $\in (1.1; 1.2)$	1806
θ_{SDSD}^F	9	prothrombin time $\in (17.7; 131.0)$ \wedge standard bicarbonate $\in (23.8; 27.3)$ \wedge sodium $\in (133.0; 141.0)$	1807
θ_{SDSD}^F	10	prothrombin time $\in (17.7; 131.0)$ \wedge blood loss $\in (0.0; 958.8)$ \wedge age $\in (51; 74)$	1808
θ_{SDSD}^F	11	prothrombin time $\in (17.7; 131.0)$ \wedge Ringer's lactate administration $\in (0.0; 4813.1)$ \wedge FIO2 $\in (0.2; 0.2)$	1809
θ_{SDSD}^F	12	prothrombin time $\in (17.7; 131.0)$ \wedge blood loss $\in (0.0; 958.8)$ \wedge fluid loss $\in (0.0; 0.0)$	1810
θ_{SDSD}^F	13	prothrombin time $\in (17.7; 131.0)$ \wedge blood loss $\in (0.0; 958.8)$ \wedge chloride $\in (105.0; 111.0)$	1811
θ_{SDSD}^F	14	prothrombin time $\in (16.5; 131.0)$ \wedge standard bicarbonate $\in (23.7; 27.3)$ \wedge potassium $\in (4.0; 5.0)$	1812
θ_{SDSD}^F	15	milrinone administration $\in (3.5; 635.4)$ \wedge cefazolin administration $\in (0.0; 92.5)$ \wedge FIO2 $\in (0.2; 0.5)$	1813

Table 15: Top-15 subgroups discovered when seeking exceptional phenotype θ_{RMSSD}^F .

Phenotype	#	Description	
θ_{RMSSD}^F	1	prothrombin time $\in (16.5; 131.0)$ \wedge standard bicarbonate $\in (23.7; 27.3)$ \wedge thrombin administration $\in (0.0; 0.0)$	1825
θ_{RMSSD}^F	2	fibrinogen $\in (1.7; 7.7)$ \wedge base excess $\in (-0.6; 7.3)$ \wedge thrombin administration $\in (0.0; 0.0)$	1826
θ_{RMSSD}^F	3	prothrombin time $\in (17.7; 131.0)$ \wedge standard bicarbonate $\in (23.8; 27.3)$ \wedge alfentanil administration $\in (0.0; 42.3)$	1827
θ_{RMSSD}^F	4	prothrombin time $\in (17.7; 131.0)$ \wedge base excess $\in (-0.7; 3.2)$ \wedge calcium ions $\in (1.1; 1.2)$	1828
θ_{RMSSD}^F	5	prothrombin time $\in (17.7; 131.0)$ \wedge cefazolin administration $\in (0.0; 90.3)$ \wedge FIO2 $\in (0.2; 0.2)$	1829
θ_{RMSSD}^F	6	prothrombin time $\in (17.7; 131.0)$ \wedge standard bicarbonate $\in (23.8; 27.3)$ \wedge calcium ions $\in (1.1; 1.2)$	1830
θ_{RMSSD}^F	7	prothrombin time $\in (16.5; 131.0)$ \wedge standard bicarbonate $\in (23.7; 27.3)$ \wedge chloride $\in (105.0; 110.0)$	1831
θ_{RMSSD}^F	8	prothrombin time $\in (17.7; 131.0)$ \wedge standard bicarbonate $\in (23.8; 27.3)$ \wedge sodium $\in (133.0; 141.0)$	1832
θ_{RMSSD}^F	9	prothrombin time $\in (17.7; 131.0)$ \wedge blood loss $\in (0.0; 958.8)$ \wedge age $\in (51; 74)$	1833
θ_{RMSSD}^F	10	milrinone administration $\in (3.5; 635.4)$ \wedge cefazolin administration $\in (0.0; 92.5)$ \wedge prothrombin time $\in (14.8; 131.0)$	1834
θ_{RMSSD}^F	11	prothrombin time $\in (17.7; 131.0)$ \wedge noradrenalin administration $\in (0.0; 24.6)$ \wedge fluid loss $\in (0.0; 0.0)$	1835
θ_{RMSSD}^F	12	prothrombin time $\in (17.7; 131.0)$ \wedge blood loss $\in (0.0; 958.8)$ \wedge fluid loss $\in (0.0; 0.0)$	1836
θ_{RMSSD}^F	13	prothrombin time $\in (17.7; 131.0)$ \wedge blood loss $\in (0.0; 958.8)$ \wedge chloride $\in (105.0; 111.0)$	1837
θ_{RMSSD}^F	14	fibrinogen $\in (1.7; 7.7)$ \wedge standard bicarbonate $\in (23.8; 30.2)$ \wedge drains $\in (0.0; 480.0)$	1838
θ_{RMSSD}^F	15	prothrombin time $\in (17.7; 131.0)$ \wedge base excess $\in (-0.7; 3.2)$ \wedge coronary artery bypass grafting = False	1839

Table 16: Top-15 subgroups discovered when seeking exceptional phenotype θ_{SDSQ}^F .

1857	1915
1858	1916
1859	1917
1860	1918
1861	1919
1862	1920
1863	1921
1864	1922
1865	1923
1866	1924
1867	1925
1868	1926
1869	1927
1870	1928
1871	1929
1872	1930
1873	1931
1874	1932
1875	1933
1876	1934
1877	1935
1878	1936
1879	1937
1880	1938
1881	1939
1882	1940
1883	1941
1884	1942
1885	1943
1886	1944
1887	1945
1888	1946
1889	1947
1890	1948
1891	1949
1892	1950
1893	1951
1894	1952
1895	1953
1896	1954
1897	1955
1898	1956
1899	1957
1900	1958
1901	1959
1902	1960
1903	1961
1904	1962
1905	1963
1906	1964
1907	1965
1908	1966
1909	1967
1910	1968
1911	1969
1912	1970
1913	1971
1914	1972